Nonperturbative functional renormalization group for random field models and related disordered systems. II. Results for the random field $O(N)$ model

Matthieu Tissier* and Gilles Tarjus†
LPTMC, CNRS-UMR 7600, Université Pierre et Marie Curie, Boîte Postale 121, 4 Place Jussieu, 75252 Paris Cedex 05, France
(Received 16 January 2008; published 9 July 2008)

We study the critical behavior and phase diagram of the d-dimensional random field $O(N)$ model by means of the nonperturbative functional renormalization group approach presented in the preceding paper. We show that the dimensional-reduction predictions, which are obtained from conventional perturbation theory, break down below a critical dimension $d_{\mathrm{DR}}(N)$ and we provide a description of criticality, ferromagnetic ordering, and quasi-long range order in the whole (N,d) plane. Below $d_{\mathrm{DR}}(N)$, our formalism gives access to both the typical behavior of the system, which is controlled by zero-temperature fixed points at which the effective action has a nonanalytic field dependence, and to the physics of rare low-energy excitations ("droplets"), which is described at nonzero temperature by the rounding of the nonanalyticity in a thermal boundary layer.

DOI: 10.1103/PhysRevB.78.024204 PACS number(s): 11.10.Hi, 75.40.Cx

I. INTRODUCTION

The random field model describes one of the simplest disordered systems in which classical N-component variables (spins in magnetic language) with $O(N)$ symmetric interactions are linearly coupled to a random (magnetic) field. Yet, more than 30 years after the first studies of the model,[1–3] its long-distance behavior (criticality and ordering) still largely appears as a puzzle.

The two main questions raised about the (equilibrium) properties concern the nature and the characteristics of the phases and of the phase transitions. The first one is about the so-called "dimensional-reduction" property that relates the critical behavior of the random field $O(N)$ model [RF$O(N)$M] in dimension d to that of the pure $O(N)$ model in dimension $d-2$. This property, which is predicted to all orders by conventional perturbation theory[2–4] and derived as a consequence of a hidden supersymmetry,[5] is known to break down in low enough dimensions.[6,7] The second question concerns the existence of a phase with quasi-long range order (QLRO) (i.e., a phase characterized by no magnetization and a power-law decrease of the correlation functions) in the models with a continuous symmetry ($N>1$) below $d=4$, which is their lower critical dimension for long-range ferromagnetism. More specifically, the presence of QLRO in the three-dimensional RFXYM ($N=2$) is of relevance to the "Bragg-glass" phase discussed in the context of vortices in disordered type-II superconductors.[8–12]

In the preceding article,[13] denoted as paper I in the following, we have developed a *nonperturbative functional renormalization group* (NP-FRG) formalism to study the long-distance physics of random field models and related disordered systems. In the present paper, we set the formalism to use to address the issues mentioned above, which concern the behavior of the RF$O(N)$M.

We start in Sec. II by briefly recalling the main definitions, notations, and results of the NP-FRG approach to the RF$O(N)$M, which was presented in paper I. Next, in Sec. III, we discuss the mechanism by which dimensional reduction breaks down, namely, the appearance of a strong enough nonanalytic behavior in the dependence of the effective average action in the dimensionless fields. We first recall the analysis of the perturbative functional renormalization group (RG) at one loop near $d=4$. We then present the scenario for the failure of dimensional reduction in the random field Ising model (RFIM) within our NP-FRG approach and extend our considerations to the whole (N,d) plane.

The numerical results obtained from our minimal truncation of the NP-FRG for the RF$O(N)$M are presented in Sec. IV. This allows us to provide a unified description of criticality, ferromagnetism, and QLRO in the whole N-d diagram. We show that two nontrivial critical lines characterize the long-distance behavior of the RF$O(N)$M [on top of the upper, $d_{\mathrm{uc}}=6$, and lower, $d_{\mathrm{lc}}(N=1)=2$ and $d_{\mathrm{lc}}(N>1)=4$, critical dimensions for the paramagnetic to ferromagnetic transition]: a line $d_{\mathrm{DR}}(N)$ separating a region of the (N,d) plane in which the critical exponents are given by the dimensional-reduction predictions [$d>d_{\mathrm{DR}}(N)$] from a region where dimensional reduction is fully broken [$d<d_{\mathrm{DR}}(N)$]; and a line $d_{\mathrm{lc}}(N)$ characterizing the lower critical dimension for quasi-long range order (for $1<N\leq N_c=2.83\cdots$). Finally, we discuss the accuracy and reliability of the present truncation.

In Sec. V, we address the physical meaning of the nonanalyticity (in the effective action), which is associated with dimensional-reduction failure. We also examine the role of temperature and the connection with the phenomenological droplet approach. In particular, we discuss the "activated dynamic scaling" behavior that characterizes the critical slowing down of relaxation in the RFIM.

We finally conclude by considering the relation of the present to other pictures of the behavior of random field models and providing some perspectives. Short accounts of the present work have already been reported in Refs. 14 and 15.

II. NONPERTURBATIVE FUNCTIONAL RENORMALIZATION GROUP APPROACH FOR THE RF$O(N)$M

The NP-FRG approach developed in paper I combines three main ingredients.

(1) A version of Wilson's continuous RG in which one follows the evolution of the effective average action Γ_k with a (momentum) scale k from the bare action at the microscopic scale ($k=\Lambda$) to the full effective action at macroscopic scale ($k=0$); the evolution of Γ_k, which is the generating functional of the one-particle irreducible vertices at scale k, is governed by an exact RG flow equation.[16]

(2) A replica formalism in which the permutational symmetry among replicas is explicitly broken by the introduction of linear sources independently acting on each replica; using an expansion in the number of unconstrained (or "free") replica sums gives access to a description of the probability distribution of the renormalized disorder through its cumulants.

(3) A nonperturbative approximation scheme for the effective average action that relies on truncating both its "derivative expansion" (expansion in number of spatial derivatives of the fundamental fields) and the "expansion in number of free replica sums" (or, equivalently, the cumulant expansion).

For the RF$O(N)$M, the minimal truncation of Γ_k, which already contains the key features for a nonperturbative study of the long-distance physics, is the following:

$$\Gamma_k\{[\phi_a]\} = \int_x \left\{ \frac{1}{2}\sum_{a=1}^{n} Z_{m,k}|\partial\phi_a(\boldsymbol{x})|^2 + \sum_{a=1}^{n} U_k(\phi_a(\boldsymbol{x})) - \frac{1}{2}\sum_{a,b=1}^{n} V_k(\phi_a(\boldsymbol{x}),\phi_b(\boldsymbol{x})) \right\}, \tag{1}$$

where as before ϕ_a, $a=1,\ldots,n$, are the replica fields, $Z_{m,k}$ is a wave function renormalization parameter, U_k is the one-replica potential that physically represents a coarse-grained Gibbs free energy and gives access to the thermodynamics of the system, and V_k is the two-replica potential that is the second cumulant of the renormalized disorder (evaluated for uniform fields).

The flow equations for $U_k(\phi_1)$, $V_k(\phi_1,\phi_2)$, and $Z_{m,k}$ are obtained from the exact RG equation for the effective average action,[13,16]

$$\partial_k\Gamma_k[\{\phi_a\}] = \frac{1}{2}\int_{\boldsymbol{q}} \mathrm{Tr}\{\partial_k \boldsymbol{R}_k(q^2)[\boldsymbol{\Gamma}_k^{(2)} + \boldsymbol{R}_k]^{-1}_{\boldsymbol{q},-\boldsymbol{q}}\}, \tag{2}$$

where the trace involves a sum over both replica indices and N-vector components and $\boldsymbol{\Gamma}_k^{(2)}$ is the tensor formed by the second functional derivatives of Γ_k with respect to the fields $\phi_a^\mu(\boldsymbol{q})$. $\boldsymbol{R}_k(q^2)$ is the infrared cutoff that enforces the decoupling of the low- and high-momentum modes at the scale k. It is diagonal in N-vector indices, and in the minimal truncation, we have also chosen it diagonal in replica indices, i.e., $R^{\mu\nu}_{k,ab}(q^2)=\hat{R}_k(q^2)\,\delta_{ab}\delta_{\mu\nu}$.

The initial condition is given by the bare replicated action of the RF$O(N)$M,

$$S[\{\phi_a\}] = \int_x \left\{ \frac{1}{2T}\sum_{a=1}^{n}\left[|\partial\phi_a(\boldsymbol{x})|^2 + \tau|\phi_a(\boldsymbol{x})|^2 + \frac{u}{12}(|\phi_a(\boldsymbol{x})|^2)^2 \right] - \frac{\Delta}{2T^2}\sum_{a,b=1}^{n}\phi_a(\boldsymbol{x})\cdot\phi_a(\boldsymbol{x}) \right\}, \tag{3}$$

where we have made explicit the dependence on a "bare" temperature T. One more step is needed to cast the NP-FRG flow equations in a form suitable for searching for the anticipated zero-temperature fixed points of the RF$O(N)$M,[17,18] namely, to introduce appropriate scaling dimensions. This requires us to define a renormalized temperature T_k that is expected to flow to zero as $k\to 0$. Near a zero-temperature fixed point, one has the following scaling dimensions:

$$T_k \sim k^\theta, \quad Z_{m,k}\sim k^{-\eta}, \quad \phi_a^\mu \sim k^{(1/2)(d-4+\bar{\eta})}, \tag{4}$$

with θ and $\bar{\eta}$ related through $\theta=2+\eta-\bar{\eta}$, as well as

$$U_k \sim k^{d-\theta}, \quad V_k \sim k^{d-2\theta}, \tag{5}$$

so that the second cumulant of the renormalized random field,

$$\Delta_k^{\mu\nu}(\phi_1,\phi_2) = \frac{\partial^2 V_k(\phi_1\phi_2)}{\partial\phi_1^\mu\,\partial\,\phi_2^\nu}, \tag{6}$$

scales as $k^{-(2\eta-\bar{\eta})}$. (We recall that the superscripts with Greek letters denote the components of the N-vector fields.)

The dimensionless counterparts of U_k, V_k, Δ_k, ϕ are denoted by lower-case letters, u_k, v_k, δ_k, $\boldsymbol{\varphi}$. [For the RF$O(N)$M, a convenient parametrization of the one- and two-replica functions makes use of the variables $\rho=|\boldsymbol{\varphi}|^2/2$ and $z=\boldsymbol{\varphi}_1\cdot\boldsymbol{\varphi}_2/\sqrt{4\rho_1\rho_2}$.] The resulting flow equations in scaled form have been given in Sec. IV of paper I.

We conclude this brief recapitulation of the results of paper I by recalling that the minimal nonperturbative truncation described above reduces to the one-loop perturbative results near the upper critical dimension $d=6$ and when $N\to\infty$, and, most importantly, that it reproduces the one-loop perturbative functional renormalization group (FRG) equations near the lower critical dimension for ferromagnetism in the $[O(N>1)]$ model, $d=4$.

III. BREAKDOWN OF DIMENSIONAL REDUCTION

As stressed in Sec. I, dimensional reduction for the random field model must break down in low enough dimension. Within the NP-FRG, we find that the mechanism by which this occurs is the appearance along the RG flow of a nonanalyticity in the dependence of the effective average action in the dimensionless fields; more precisely, the appearance of a cusp in the second cumulant of the renormalized random field as one makes the two field arguments approach each other. The theory is renormalizable, although with the unusual feature that the renormalized effective action is nonanalytic at the fixed point. Such a mechanism has previously been found in the random manifold model within the perturbative FRG approach.[19–23]

In this section, we discuss the appearance of a nonanalytic behavior within our minimal truncation scheme. We first recall the results obtained near $d=4$ for the RF$O(N>1)$M,[14,24–26] since this limit is more easily accessible to an analytic treatment and already provides the scenario for the general case.

A. RF$O(N)$M at one loop near $d=4$

Our starting point is the set of equations derived at first order in $\epsilon=d-4$ and at zero temperature for the running exponents η_k, $\bar{\eta}_k$ and for the dimensionless renormalized second cumulant of the disorder, more precisely for $R_k(z)=v_k(\rho_{m,k},\rho_{m,k},z)/(2\rho_{m,k})^2$, where $\rho_{m,k}$ corresponds to the minimum of the one-replica potential (i.e., is akin to a dimensionless order parameter at the running scale k) and goes as $1/\epsilon$ at the relevant fixed points [see Eqs. (100) and (101) of paper I]. [Note that $R_k(z)$ should not be confused with the regulator $\mathbf{R}_k(q^2)$ that appears for instance in Eq. (2).] For studying the fixed points and their stability, it is convenient to introduce $\tilde{R}_k(z)=(4v_4/\epsilon)R_k(z)$ and to rescale the RG "time" as $\epsilon t\to t$. The flow equation then reads

$$\begin{aligned}\partial_t\tilde{R}_k(z) &= \tilde{R}_k(z) - 2(N-2)\tilde{R}_k'(1)\tilde{R}_k(z) \\ &\quad - \frac{1}{2}(N-1)[\tilde{R}_k'(z) - 2z\tilde{R}_k'(1)]\tilde{R}_k'(z) \\ &\quad - \frac{1}{2}(1-z^2)\{-\tilde{R}_k'(z)^2 + 2[\tilde{R}_k'(1) - z\tilde{R}_k'(z)]\tilde{R}_k''(z) \\ &\quad + (1-z^2)\tilde{R}_k''(z)^2\},\end{aligned} \tag{7}$$

where $t=\ln(k/\Lambda)$, and one also has

$$\eta_k = \epsilon\tilde{R}_k'(1), \quad \bar{\eta}_k = \epsilon[(N-1)\tilde{R}_k'(1) - 1]. \tag{8}$$

It is instructive to start by analyzing the flow equations for the first derivatives $\tilde{R}_k'(z=1)$ and $\tilde{R}_k''(z=1)$, assuming that $\tilde{R}_k(z)$ is at least twice continuously differentiable around $z=1$. These equations read

$$-\partial_t\tilde{R}_k'(1) = -\tilde{R}_k'(1) + (N-2)\tilde{R}_k'(1)^2, \tag{9}$$

$$-\partial_t\tilde{R}_k''(1) = [-1 + 6\tilde{R}_k'(1)]\tilde{R}_k''(1) + (N+7)\tilde{R}_k''(1)^2 + \tilde{R}_k'(1)^2. \tag{10}$$

If $\tilde{R}_k(z)$ is analytic around $z=1$, the flow equations for the higher derivatives evaluated in $z=1$ can be derived as well. As noted by Fisher,[24] the expression for the pth derivative only involves derivatives of lower or equal order. This structure allows an iterative solution of the fixed-point equations obtained by setting the left-hand sides to zero, provided of course that $\tilde{R}_*(z)$ has the required analytic property.

Beside the stable fixed point $\tilde{R}_*'(1)=0$, there is one nontrivial fixed point associated with Eq. (9),

$$\tilde{R}_*'(1) = 1/(N-2), \tag{11}$$

with a positive eigenvalue $\Lambda_1=\epsilon$. This fixed point leads to the dimensional-reduction value of the critical exponents, i.e., $\eta=\bar{\eta}=\epsilon/(N-2)$ and $\nu=1/\Lambda_1=1/\epsilon$. On the other hand, Eq. (10) has nontrivial fixed-point solutions only when $N\geq 18$. These solutions are

$$\tilde{R}_*''(1) = \frac{(N-8)+\sqrt{(N-2)(N-18)}}{2(N-2)(N+7)}, \tag{12}$$

which is unstable with an eigenvalue $\Lambda_2=\sqrt{(N-18)/(N-2)}\epsilon$, and

$$\tilde{R}_*''(1) = \frac{(N-8)-\sqrt{(N-2)(N-18)}}{2(N-2)(N+7)}, \tag{13}$$

which is stable with $\Lambda_2=-\sqrt{(N-18)/(N-2)}\epsilon$. For $N<18$, no fixed-point solutions exist for Eq. (10). One instead finds that there is a (finite) range of initial conditions $\tilde{R}_\Lambda'(1)$ for which the RG flow for $\tilde{R}_k''(1)$ leads to a divergence at a *finite* scale k, irrespective of the initial value $\tilde{R}_\Lambda''(1)$.

The solution to the absence of a nontrivial, twice differentiable fixed-point function $\tilde{R}_*(z)$ when $N<18$, is that the proper fixed point controlling the critical behavior is nonanalytic around $z=1$, with $\tilde{R}_*'(z)$ having a cusp, i.e., a term proportional to $\sqrt{1-z}$ when $z\to 1$. Numerical solutions showing this cuspy behavior have been given by Feldman[25] for $N=3,4,5$ and by us for general values of $N<18$.[14]

We showed in detail in Ref. 26 that the value $N_{\rm DR}=18$ separates a region in which $\tilde{R}_*'(z)$ at the critical, i.e., once unstable, fixed point has a cusp ($N<N_{\rm DR}$) from a region ($N>N_{\rm DR}$), where $\tilde{R}_*'(z)$ has only a weaker nonanalyticity, a "subcusp" in $(1-z)^{\alpha(N)}$ with $\alpha(N)$ being a noninteger larger than 3/2. The occurrence of a cusp changes the values of η and $\bar{\eta}$ from the dimensional-reduction prediction, $\eta_{\rm DR}=\bar{\eta}_{\rm DR}=\epsilon/(N-2)$. Indeed, the flow equation for $\tilde{R}_k'(1)$ is modified according to

$$\begin{aligned}-\partial_t\tilde{R}_k'(1) &= -\tilde{R}_k'(1) + (N-2)\tilde{R}_k'(1)^2 \\ &\quad + \lim_{z\to 1}\{2(1-z)\tilde{R}_k''(z)[2(1-z)\tilde{R}_k'''(z) - 3\tilde{R}_k''(z)] \\ &\quad + [(N+1)\tilde{R}_k''(z) - 2(1-z)\tilde{R}_k'''(z)] \\ &\quad \times(\tilde{R}_k'(z) - \tilde{R}_k'(1))\},\end{aligned} \tag{14}$$

where the whole term $\lim_{z\to 1}(\cdots)$ is nonzero when a cusp is present in $\tilde{R}_k'(z)$. As a result, the once unstable fixed-point solution for $\tilde{R}_*'(1)$ is no longer equal to $1/(N-2)$ and it follows from Eqs. (8) that dimensional reduction is broken.[27]

On the other hand, the weaker nonanalyticity occurring for $N>18$ does not alter the flow equation for $\tilde{R}_k'(1)$, which is still given by Eq. (9), and dimensional reduction still applies; in particular, $\eta=\bar{\eta}=\eta_{\rm DR}$. This drastic change in behavior at $N=18$ is illustrated in Fig. 1, where $\eta_{\rm DR}/\eta$ and $\bar{\eta}_{\rm DR}/\bar{\eta}$ are plotted as a function of N.

To gain some insight into the order of the nonanalyticity, one may analyze the hierarchy of flow equations for the successive derivatives of $\tilde{R}_k(z)$ evaluated in $z=1$.[24,26] As ex-

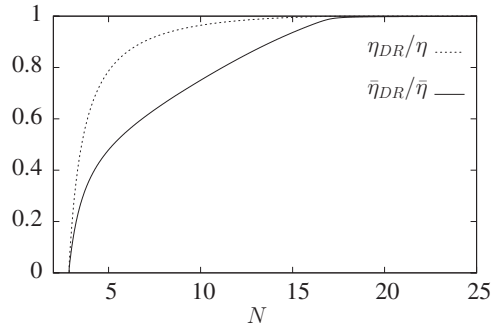

FIG. 1. Breakdown of dimensional reduction near $d=4$: η_{DR}/η (lower curve) and $\bar{\eta}_{\mathrm{DR}}/\bar{\eta}$ (upper curve) versus N for the RF$O(N)$M with $N\geq 3$ at first order in $\epsilon=d-4$. The dimensional-reduction value of the exponents is $\eta_{\mathrm{DR}}=\bar{\eta}_{\mathrm{DR}}=\epsilon/(N-2)$.

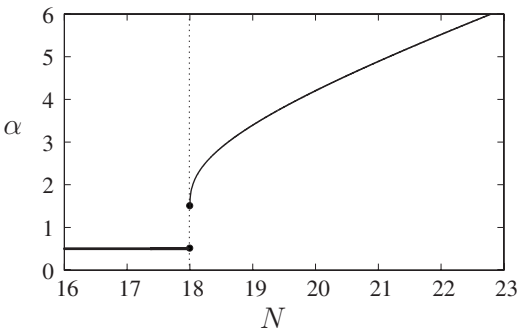

FIG. 2. Exponent $\alpha(N)$ characterizing the order of the nonanalyticity in the cumulant of the renormalized random field, $R'(z)$, near $z=1$ for the RF$O(N)$M in $d=4+\epsilon$. A cusp leading to breakdown of dimensional reduction corresponds to $\alpha(N)=1/2$ and is obtained for $N<18$. There is a discontinuity at $N=18$ with $\alpha(N=18^{+})=3/2$.

plained above, a fixed point with a well-defined second derivative and an associated negative eigenvalue ($\Lambda_2<0$) can be found for $N>18$ [see Eq. (13)].[28]

Let us assume that the first p derivatives of $\tilde{R}_k(z)$ are well defined in $z=1$. Contrary to the flow equations for $\tilde{R}_k'(1)$ and $\tilde{R}_k''(1)$ [see Eqs. (9) and (10)], those for the higher derivatives are linear, namely,

$$-\partial_t \tilde{R}_k^{(p)}(1) = \Lambda_p[\tilde{R}_k'(1),\tilde{R}_k''(1)]\tilde{R}_k^{(p)}(1) + \mathcal{F}_p[\tilde{R}_k'(1),\tilde{R}_k''(1),\cdots,\tilde{R}_k^{(p-1)}(1)], \quad (15)$$

where Λ_p and $\mathcal{F}_p$ are known functions easily derived from Eq. (7). If $\tilde{R}_k'(1)$ and $\tilde{R}_k''(1)$ are chosen equal to their fixed-point values given in Eqs. (11) and (13), one finds that

$$\Lambda_{p*} = \frac{\epsilon}{N-2}\left[2p^2-(N-1)p+(N-2) + \frac{p(N-5+6p)}{2(N+7)}(N-8-\sqrt{(N-2)(N-18)})\right]. \quad (16)$$

For a given N, there exists an integer value $p_{\#}(N)$ such that $\Lambda_{p*}<0$ for $p\leq p_{\#}(N)$ and $\Lambda_{p*}>0$ for $p\geq p_{\#}(N)+1$. The RG flow for the $[p_{\#}(N)+1]$th derivative therefore diverges when $t\to-\infty$, whereas all lower-order derivatives reach finite fixed-point values. As a consequence, the fixed-point function $\tilde{R}_*'(z)$ must have a nonanalyticity of the form $(1-z)^{\alpha(N)}$ with $p_{\#}(N)-1<\alpha(N)<p_{\#}(N)$. Refining the reasoning,[26] one finds that $\alpha(N)$ is given by the solution of $\Lambda_{\alpha(N)+1*}=0$, where $\Lambda_{\alpha(N)+1*}$ is given by Eq. (16) with p replaced by the noninteger $\alpha(N)+1$. The result is shown in Fig. 2: the order of the nonanalyticity increases with N when $N>18$, which starts from 3/2 when $N\to 18^{+}$, and it goes as $N/2+O(1)$ at large N.

Finally, we stress the different ways in which "cusp" and "subcusps" appear along the RG flow. As seen above, subcusps occur only at infinite RG time (i.e., at the fixed point). On the contrary, due to the nonlinear nature of the beta function for $\tilde{R}_k''(1)$ [see Eq. (10)], a cusp appears at a finite time, which one may define as a "Larkin scale" by analogy with the behavior of disordered elastic systems.[22,23,29,30]

B. Analytic versus nonanalytic behavior in the random field Ising model

Consider now the Ising version of the random field model at zero temperature. We saw in Sec. IV B of paper I that "anomalous" contributions to the combination of running exponents $2\eta_k-\bar{\eta}_k$ may appear if the dimensionless renormalized cumulant $\delta_k(\varphi_1,\varphi_2)$ becomes nonanalytic as the two field arguments approach each other, $\varphi_2\to\varphi_1$. This can be more conveniently studied by changing the variables to $x=(\varphi_1+\varphi_2)/2$ and $y=(\varphi_1-\varphi_2)/2$; the dependence of δ_k on x is anticipated as being completely regular and that on y as potentially anomalous. (Recall that due to the Z_2 and permutational symmetries, δ_k is even in x and y separately.) The flow equation for $\delta_k(x,y)$ is obtained from that for $v_k(\varphi_1,\varphi_2)$ given in paper I by deriving with respect to φ_1 and φ_2 and switching to the new variables x and y. One finds that

$$\begin{aligned}\partial_t\delta_k(x,y) = {} & (2\eta-\bar{\eta})\delta(x,y)+\frac{1}{2}(d-4+\bar{\eta})(x\partial_x+y\partial_y)\delta(x,y) - v_d\left\{\frac{1}{2}[l_2^{(d)}(w_+)\delta_{0+}+l_2^{(d)}(w_-)\delta_{0-}-2l_{1,1}^{(d)}(w_+,w_-)\delta(x,y)]\delta^{(02)}(x,y)\right.\\
& -l_{1,1}^{(d)}(w_+,w_-)\delta^{(01)}(x,y)^2+[[l_2^{(d)}(w_+)\delta_{0+}'-l_2^{(d)}(w_-)\delta_{0-}']+2[l_{2,1}^{(d)}(w_+,w_-)w_+'-l_{1,2}^{(d)}(w_+,w_-)w_-']\delta(x,y)-2[l_3^{(d)}(w_+)w_+'\delta_{0+}\\
& -l_3^{(d)}(w_-)w_-'\delta_{0-}]]\delta^{(01)}(x,y)+[l_2^{(d)}(w_+)\delta_{0+}-l_2^{(d)}(w_-)\delta_{0-}]\delta^{(11)}(x,y)+2l_{2,2}^{(d)}(w_+,w_-)w_+'w_-'\delta(x,y)^2+l_{1,1}^{(d)}(w_+,w_-)\delta^{(10)}(x,y)^2\\
& +[[l_2^{(d)}(w_+)\delta_{0+}'+l_2^{(d)}(w_-)\delta_{0-}']-2[l_3^{(d)}(w_+)w_+'\delta_{0+}+l_3^{(d)}(w_-)w_-'\delta_{0-}]-2[l_{2,1}^{(d)}(w_+,w_-)w_+'+l_{1,2}^{(d)}(w_+,w_-)w_-']\delta(x,y)]\delta^{(10)}(x,y)\\
& \left.+\frac{1}{2}[l_2^{(d)}(w_+)\delta_{0+}+l_2^{(d)}(w_-)\delta_{0-}+2l_{1,1}^{(d)}(w_+,w_-)\delta(x,y)]\delta^{(20)}(x,y)\right\}, \quad (17)\end{aligned}$$

where we have dropped the subscript k on the right-hand side and introduced the short-hand notation $w_{\pm}=u_k''(x\pm y)$ and $\delta_{0\pm}=\delta_{k,0}(x\pm y)$ with $\delta_{k,0}(x)=\delta_k(x,y=0)$; for a function of a single argument, a prime denotes a derivative, whereas for functions of two arguments, partial derivatives are indicated as superscripts, e.g., $\delta^{(10)}(x,y)=\partial_x\delta(x,y)$, $\delta^{(01)}(x,y)=\partial_y\delta(x,y)$, etc. Finally, $l_n^{(d)}(w)$ and $l_{n_1,n_2}^{(d)}(w_1,w_2)$ are the "dimensionless threshold functions" defined from the infrared cutoff function $\hat{R}_k(q^2)=Z_k q^2 r(q^2/k^2)$ (see paper I and Ref. 16).

We now follow a reasoning similar to that developed for the RF$O(N)$M near $d=4$. Assume that $\delta_k(x,y)$ is continuously differentiable with respect to y around $y=0$ up to some order $2p$ with $p\geq 1$. Then, introducing the notation $\delta_{k,q}(x)=\partial_y^q\delta_k(x,y)|_{y=0}$ and using the property that all derivatives of odd order vanish in $y=0$ due to the inversion symmetry, one may express $\delta_k(x,y)$ in the vicinity of $y=0$ as

$$\delta_k(x,y)=\sum_{q=0}^{p}\frac{y^{2q}}{(2q)!}\delta_{k,2q}(x)+o(y^{2p}). \tag{18}$$

By inserting this expression in the RG flow equation for $\delta_k(x,y)$ [Eq. (17)], one derives the following flow equations for the function evaluated in $y=0$:

$$\begin{aligned}\partial_t\delta_{k,0}(x)=&(2\eta_k-\bar{\eta}_k)\delta_{k,0}(x)+\frac{1}{2}(d-4+\bar{\eta}_k)x\delta_{k,0}'(x)\\&-2v_d\Big\{l_4^{(d)}(u_k''(x))\delta_{k,0}(x)^2u_k'''(x)^2\\&-4l_3^{(d)}(u_k''(x))u_k'''(x)\delta_{k,0}(x)\delta_{k,0}'(x)\\&+l_2^{(d)}(u_k''(x))\left[\frac{3}{2}\delta_{k,0}'(x)^2+\delta_{k,0}(x)\delta_{k,0}''(x)\right]\Big\},\end{aligned} \tag{19}$$

and for the derivatives,

$$\begin{aligned}\partial_t\delta_{k,2}(x)=&-L_2[u_k'',\delta_{k,0}]\delta_{k,2}(x)+3v_dl_2^{(d)}(u_k''(x))\delta_{k,2}(x)^2\\&-2v_d\mathcal{G}_2[u_k'',\delta_{k,0}],\end{aligned} \tag{20}$$

and for $p\geq 2$,

$$\begin{aligned}\partial_t\delta_{k,2p}(x)=&-L_{2p}[u_k'',\delta_{k,0},\delta_{k,2}]\delta_{k,2p}(x)\\&-2v_d\mathcal{G}_{2p}[u_k'',\{\delta_{k,2q}\}_{q\leq p-1}],\end{aligned} \tag{21}$$

where $L_2[u_k'',\delta_{k,0}]$ and $L_{2p}[u_k'',\delta_{k,0},\delta_{k,2}]$ are linear operators whose expressions are given in Appendix A. The $\mathcal{G}_{2p}$'s are functionals of $u_k''(x)$ and $\delta_{k,0}(x)$ and of the derivatives $\delta_{k,2q}(x)$ with $q\leq p-1$. Their expressions are not worth displaying.

The above equations are complemented by the flow equation for $u_k(x)$, or its derivative $u_k'(x)$, which are obtained from the results of Sec. IV B in paper I,

$$\begin{aligned}\partial_t u_k'(x)=&-\frac{1}{2}(d+\bar{\eta}_k-2\eta_k)u_k'(x)+\frac{1}{2}(d-4+\bar{\eta}_k)xu_k''(x)\\&+2v_d\{l_1^{(d)}(u_k''(x))\delta_{k,0}'(x)-l_2^{(d)}(u_k''(x))u_k'''(x)\delta_{k,0}(x)\},\end{aligned} \tag{22}$$

and the expression for the running anomalous dimension,[13]

$$\begin{aligned}\eta_k=&\frac{8v_d}{d}\{2m_{3,2}^{(d)}(u_k''(x_{m,k}),u_k''(x_{m,k}))u_k'''(x_{m,k})^2\\&-m_{2,2}^{(d)}(u_k''(x_{m,k}),u_k''(x_{m,k}))u_k'''(x_{m,k})\},\end{aligned} \tag{23}$$

where $x_{m,k}$ denotes the nontrivial configuration that minimizes the one-replica potential, and which therefore satisfies $u_k'(x_{m,k})=0$; the $m_{n_1,n_2}^{(d)}(w_1,w_2)$'s are additional dimensionless threshold functions (see paper I and Ref. 16). Similarly, one also has an expression for $2\eta_k-\bar{\eta}_k$, which is derived from Eqs. (19) and (22) and the constraint $\delta_{k,0}(x_{m,k})=1$ (one recovers the equation of paper I, but now without the anomalous terms).

One first notices that the RG equations for $u_k'(x)$, $\delta_{k,0}(x)$, and η_k form a closed set. No additional input is required from the derivatives $\delta_{k,2p}(x)$ with $p\geq 1$, which means that the RG flow for the one-replica potential and for the two-replica potential (or the second cumulant) evaluated for equal field arguments is closed without further knowledge of the full field dependence of the two-replica potential for distinct replicas. This property is a direct consequence of the assumption that the behavior of the second cumulant is sufficiently regular when the two field arguments become equal, more precisely, that $\partial_y^2\delta_k(x,y)$ is finite when $y\to 0$.

Before discussing the consequences of this property, it is worth mentioning that it results from the structure of the exact RG equations and not from the specific approximation chosen here. More generally indeed, the exact RG flows for the one-replica component of the effective average action and for the cumulants of the renormalized random field (see Secs. IIC and IID of paper I) evaluated for equal field arguments decouple from the full functional dependence of the cumulants when the latter is regular enough in the limit of equal arguments. This point will be further developed and clarified in a forthcoming publication centered on the superfield formalism.[31]

As in the previously discussed case of the RF$O(N)$M near $d=4$, one expects that the fixed point obtained without reference to distinct replicas, and associated with a regular enough behavior of the cumulants in the limit of equal arguments, corresponds to dimensional reduction. To prove this, one needs to show that it is equivalent, in the one-replica sector at least, to the corresponding fixed point of the pure system in two dimensions less. This is indeed illustrated near the upper critical dimension $d=6$: it is easy to show (see also Sec. IVD of paper I) that, at first order in $\epsilon=6-d$, Eqs. (19), (22), and (23) give back the result of the pure Ising model at first order in $\epsilon=4-d$. The difficulty in going beyond this step is that the present truncation may explicitly break the supersymmetry discussed in Ref. 5. For instance, the terms of second order in $\epsilon=6-d$ of Eqs. (19), (22), and (23) break the dimensional-reduction property; however, this is clearly an

artifact of the truncation and of the choice of regulator. One can check this by improving the treatment so that the exact two-loop results are recovered near $d=6$: the calculation becomes extremely tedious in the present formalism and a nonperturbative closure becomes hardly tractable numerically; but it is nonetheless found by a direct analysis near $d=6$ that if the two- and three-replica cumulants are regular enough in their field dependence so that the flow equations evaluated for equal replica fields decouple as in Eqs. (19), (22), and (23), the corresponding fixed point at second order in ϵ leads to dimensional reduction.

Awaiting a proper resolution of the problem via the superfield formalism,[31] we will associate with dimensional reduction the fixed point corresponding to Eqs. (19), (22), and (23), fixed point that can be continuously followed as a function of dimension d and, as will be discussed below, as a function of the number of components N. Breaking of dimensional reduction therefore implies the occurrence of a strong enough nonanalyticity in the field dependence of the renormalized cumulants of the disorder. Here, "strong enough" means that it is sufficient to couple the flow of the components of the effective average action evaluated for equal fields to the full functional dependence involving distinct replica fields.

From the flow equation for $\delta_k(\varphi_1,\varphi_2)\equiv\delta_k(x,y)$ [Eq. (17)], it is clear that the only way to avoid dimensional reduction is therefore the existence of a linear cusp in the fixed-point function $\delta_*(x,y)$, i.e., with

$$\delta_*(x,y)=\delta_{*,0}(x)+|y|\delta_{*,a}(x)+O(y^2), \tag{24}$$

in the vicinity of $y=0$. This leads to the appearance of an anomalous contribution to the expression of the beta function for $\delta_{k,0}(x)$,

$$\beta_{\delta_0}(x)=\beta_{\delta_0}|_{\mathrm{reg}}(x)-v_d l_2^{(d)}(u_*''(x))\delta_{*,a}(x)^2, \tag{25}$$

where $-\beta_{\delta_0}|_{\mathrm{reg}}(x)$ is given by the right-hand side of Eq. (19). The above equation gives back the expression of $2\eta_k-\bar{\eta}_k$ derived in Sec. IVB of paper I with the temperature set to zero.

Before closing this discussion of the RFIM, we would like to emphasize a few additional points that parallel the comments made in Sec. III A. First, the appearance of a cusp in $\delta_k(x,y)$ is associated with the divergence of the second derivative $\delta_{k,2}(x)$. Due to the nonlinear character of the flow equation for $\delta_{k,2}(x)$ [Eq. (20)], this divergence, if present, is expected to first occur at a finite scale which, as before, we generically call the Larkin scale. For a running scale k larger than the Larkin scale k_L, the effective average action is analytic and it develops a cusp [in $\delta_k(x,y)$] for k less than k_L. From the flow equation for $\delta_k(x,y)$, one can see that a linear cusp is stable under RG flow, in that it does not lead to stronger "supercusps."

Second, the appearance of a subcusp in $\delta_k(x,y)$ is signaled by the divergence of a higher-order derivative $\delta_{k,2p}(x)$, with $p\geq 2$ being related to the order of the nonanalyticity [which is strictly less than $2p$ and strictly more than $2(p-1)$]. The flow equation for $\delta_{k,2p}(x)$ being linear, a subcusp can only appear at infinite RG time, i.e., at the fixed point. Following the reasoning developed in Appendix A, we conclude that the order of the nonanalyticity characterizing the fixed point increases as $1/(6-d)^2$ when d approaches 6 from below. This is the counterpart of the situation found near $d=4$ where the order of the nonanalyticity increases as $N/2$ when the number of components N gets large. In both cases, the critical fixed points with fully analytic effective action (as a function of dimensionless fields) found above $d=6$ and when $N\to\infty$ are approached in d or N by fixed points with diverging orders of the nonanalyticity, i.e., with weaker and weaker subcusps. We recall, however, that such subcusps are not sufficient to break dimensional reduction.

C. Extension to the whole (N,d) plane

The preceding developments on the connection between breakdown of dimensional reduction and nonanalyticity of the effective average action can be extended to the whole (N,d) plane. The nonanalyticity now occurs in the renormalized cumulants of the disorder as two arguments, i.e., two replica fields, approach each other, $\boldsymbol{\varphi}_2\to\boldsymbol{\varphi}_1$. If the nonanalyticity is weak enough, namely, if it is weaker than a linear cusp in the second cumulant of the renormalized random field, the RG flows for $u_k(\rho),\delta_{k,T}(\rho),\delta_{k,L}(\rho),\eta_k$ (see Sec. IVC of paper I) decouple from those involving distinct replica fields. The associated fixed point can be continuously followed in the (N,d) plane and, near $d=6$, near $d=4$ for $N>18$, and when $N\to\infty$, it leads to dimensional reduction. For reasons explained above, a direct proof that it corresponds to dimensional reduction away from the perturbative regime is hampered by the truncation used here, but we rely on the continuity argument within the (N,d) plane to nonetheless identify it with an approximation of the dimensional-reduction fixed point.

Breaking of dimensional reduction is thus associated with the appearance of a sufficiently strong nonanalyticity in the two-replica potential $v_k(\rho_1,\rho_2,z)$. Analysis of the flow equation for $v_k(\rho_1,\rho_2,z)$ (see paper I) shows that this corresponds to the following behavior as $\boldsymbol{\varphi}_2\to\boldsymbol{\varphi}_1$:

$$v_k(\rho_1,\rho_2,z)\simeq v_{k,\mathrm{reg}}(\rho_1,\rho_2,s^2)+|s|^3 v_{k,a}(\rho,r^2,|s|), \tag{26}$$

with $s^2=|\boldsymbol{\varphi}_1-\boldsymbol{\varphi}_2|^2/(8\sqrt{\rho_1\rho_2})$, $\rho=(\rho_1+\rho_2)/2$, $r=(\rho_1-\rho_2)/(4|s|)$, $|\boldsymbol{\varphi}_1-\boldsymbol{\varphi}_2|^2=2(\rho_1+\rho_2-2\sqrt{\rho_1\rho_2}z)$, and $v_{k,\mathrm{reg}}$ and $v_{k,a}$ are analytic functions of their arguments in the vicinity of $\rho_2=\rho_1=\rho$, $z=1$ (i.e., $s=0$), and $r^2\lesssim\rho^2$. The cusp in the second cumulant of the renormalized random field, $\delta_k^{\mu\nu}(\rho_1,\rho_2,z)=\partial_{\varphi_1^\mu}\partial_{\varphi_2^\nu}v_k(\rho_1,\rho_2,z)$, occurs in $|s|$ or, equivalently, in $|\boldsymbol{\varphi}_1-\boldsymbol{\varphi}_2|$; it is marked by the divergence of the second derivative of v_k with respect to s^2 when $s=0$ (which also implies $\rho_2=\rho_1$). Note, however, that on top of $|\boldsymbol{\varphi}_1-\boldsymbol{\varphi}_2|$, there is now an additional variable, denoted as r above, which characterizes the way $\boldsymbol{\varphi}_2$ approaches $\boldsymbol{\varphi}_1$.

To conclude this section, it should be stressed that the consistency of the present scenario and the actual occurrence of a cusp in a region of the (N,d) diagram must be verified by a numerical resolution of the NP-FRG equations. This is what we address now.

IV. UNIFIED DESCRIPTION OF CRITICALITY, FERROMAGNETISM, AND QUASI-LONG-RANGE ORDER

A. Renormalization group flow equations and their numerical resolution

The RG flow equations for the RF$O(N)$M in the minimal truncation of the NP-FRG discussed above are given in paper I. Focusing on the fixed points and their vicinity, we drop the subdominant terms involving the temperature (it will be checked that the temperature exponent θ is indeed strictly positive). The structure of the resulting equations can be summarized as follows:

$$\partial_t u'_k(\rho) = -\beta_{u'}[u'_k, \delta_{k,T}, \delta_{k,L}; \eta_k, \bar{\eta}_k](\rho), \tag{27}$$

$$\partial_t v_k(\rho_1, \rho_2, z) = -\beta_v[u'_k, v_k; \eta_k, \bar{\eta}_k](\rho_1, \rho_2, z), \tag{28}$$

$$\eta_k = \gamma_\eta(\rho_{m,k}, u''_k(\rho_{m,k}), \delta_{k,T}(\rho_{m,k}), \delta_{k,L}(\rho_{m,k})), \tag{29}$$

where $\beta_{u'}$ and β_v are functionals and γ_η is a function; $\delta_{k,T}(\rho) = (2\rho)^{-1}\partial_z v_k(\rho, \rho, z)|_{z=1}$ and $\delta_{k,L}(\rho) = 2\rho\partial_{\rho_1}\partial_{\rho_2} v_k(\rho_1, \rho_2, z=1)|_{\rho_1=\rho_2=\rho}$ are the transverse and longitudinal components of the second cumulant of the renormalized random field evaluated for equal field arguments, and $\rho_{m,k}$ is the configuration that minimizes the one-replica potential $[u'_k(\rho_{m,k})=0]$. The running exponent $\bar{\eta}_k$ is derived from the flow of the constraint $\delta_{k,T}(\rho_{m,k})=1$ that follows from the definition of the renormalized temperature.[13]

Equations (27)–(29) form a set of coupled partial differential equations involving, in particular, a function of three variables. Studying the whole (N,d) plane by numerically solving these equations remains a very difficult and computationally intensive task. To facilitate the study, we have used in addition an expansion in powers of the fields. However, some caution must be exerted in order to retain enough of the functional character for allowing a description of possible cusp or nonanalytic dependence. We have therefore considered an expansion of ρ_1, ρ_2 around the configuration $\rho_{m,k}$ while keeping the complete dependence on the variable $|\boldsymbol{\varphi}_1 - \boldsymbol{\varphi}_2|^2$ which we anticipate to be the key variable for describing the cusp (see above). More specifically, we have chosen the following approximation:

$$u_k(\rho) = \left(\frac{\lambda_k}{8}\right)(\rho - \rho_{m,k})^2, \tag{30}$$

$$v_k(\rho_1, \rho_2, z) = v_{k,00}(s^2) + v_{k,10}(s^2)(\rho_1 + \rho_2 - 2\rho_{m,k}) + \frac{1}{2}v_{k,20}(s^2) \times (\rho_1 + \rho_2 - 2\rho_{m,k})^2 + \frac{1}{2}v_{k,02}(s^2)(\rho_1 - \rho_2)^2, \tag{31}$$

where $s^2 = |\boldsymbol{\varphi}_1 - \boldsymbol{\varphi}_2|^2/(8\rho_{m,k}) = (\rho_1 + \rho_2 - 2\sqrt{\rho_1\rho_2}z)/(4\rho_{m,k})$ (when $\rho_1 = \rho_2 = \rho_{m,k}$, s^2 then varies between 0 and 1); by construction, $v'_{k,00}(0) = \delta_{k,T}(\rho_{m,k}) = 1$. It is easily checked that this truncation still reproduces the perturbative results near $d=6$, $d=4$, and when $N \to \infty$ (compare with Sec. V of paper I).

Inserting the above expressions into the flow equations [Eqs. (27)–(29)], provides a set of coupled partial differential equations for four functions, $v_{k,00}(s^2)$, $v_{k,01}(s^2)$, $v_{k,20}(s^2)$, and $v_{k,02}(s^2)$, and three running parameters, $\rho_{m,k}$, λ_k, and η_k (plus, when convenient, $\bar{\eta}_k$), whose resolution now represents a more tractable numerical problem.

We close this section by outlining the numerical methods used for solving the partial differential equations. For each couple (N,d) and for a choice of the infrared cutoff function (in most calculations, we have taken the "optimized" regulator[32] described in paper I that leads to explicit analytic expressions for all the dimensionless threshold functions appearing in the beta functions), we follow the evolution under RG flow of the various functions and parameters for given initial conditions. For the functions, a finite difference mesh is used for the variable s, so that standard algorithms are sufficient to solve the evolution with the RG time t (or equivalently, the scale k). When necessary, most notably for checking the robustness of a nonanalytic cusplike behavior around $s=0$, we vary the mesh spacing. To reach the critical, once unstable, fixed point, we fine tune the initial condition for $\rho_{m,k}$, which represents the unstable direction. We consider that a fixed point is attained when the sum of the absolute values of all beta functions is less than 10^{-6}. The whole procedure can be accelerated by following the fixed points by continuity (when possible) in the (N,d) plane through small finite changes in N and/or d. We now move on to the presentation of the main results.

B. Dimensional reduction and its breaking

To study the "weakly nonanalytic" critical fixed point associated with dimensional reduction (see Sec. III), one does not need the full dependence on s of the functions $v_{k,00}$, $v_{k,01}$, $v_{k,20}$, and $v_{k,02}$, but only their value and that of their first derivative evaluated in $s=0$. In addition, to check the stability of this fixed point to the appearance of a cusp in $|s|$ in the dimensionless cumulant of the renormalized random field δ_k (or, equivalently, a term in $|s|^3$ in v_k), we also follow the second derivative of the functions, which is evaluated in $s=0$.

We find that the dimensional-reduction fixed point is stable versus cusplike behavior in a whole region of the (N,d) plane. However, there is a critical dimension $d_{\mathrm{DR}}(N)$ depending on N [which one may as well describe for fixed d, as a critical number of components $N_{\mathrm{DR}}(d)$] at which the second derivative of v_k with respect to s^2 in $s=0$ first diverges along the RG flow at a finite Larkin scale. The difference in behavior above and below $d_{\mathrm{DR}}(N)$ is illustrated in Fig. 3. For $N=3$, we display the evolution with t of the second derivative of v_k with respect to s^2 evaluated in $\rho_1 = \rho_2 = \rho_{m,k}$ and $s=0$, i.e., up to a constant prefactor, $v''_{k,00}(0)$. The initial condition on $\rho_{m,k}$ has been fine tuned so that the other running quantities (see above) reach the dimensional-reduction fixed point. For $d=5.5$, $v''_{k,00}(0)$ reaches a finite fixed-point value; conversely, for $d=5.0$, it diverges at a finite Larkin time. [Note that the other second derivatives, $v''_{k,10}(0)$, $v''_{k,20}(0)$, and $v''_{k,02}(0)$, all diverge at the same Larkin scale.] The value of $d_{\mathrm{DR}}(N)$ in this case in about 5.1.

When $d \to 4^+$, we numerically recover the value $N_{\mathrm{DR}}=18$, thereby confirming that the nonperturbative truncation actually leads back to the perturbative FRG result near $d=4$. The

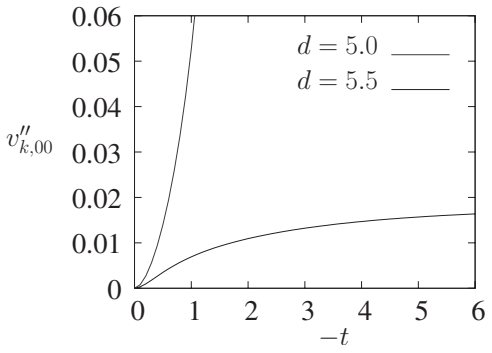

FIG. 3. Difference in behavior above and below $d_{\mathrm{DR}}(N)$ for $N=3$: evolution with RG time $|t|$ of $v''_{k,00}(0)$ which, up to a constant prefactor, is the second derivative of the dimensionless two-replica potential v_k with respect to $s^2 \propto |\varphi_1 - \varphi_2|^2$ evaluated in $\rho_1 = \rho_2 = \rho_{m,k}$ and $s=0$. The initial condition on $\rho_{m,k}$ has been fine tuned so that the other running quantities reach the dimensional-reduction fixed point. For $d=5.5$ (lower curve), $v''_{k,00}(0)$ reaches a finite fixed-point value; conversely, for $d=5.0$ (upper curve), it diverges at a finite Larkin time.

curve $N_{\mathrm{DR}}(d)$ continuously extends down to $N=1$, where we obtain $d_{\mathrm{DR}}(N) \simeq 5$. It separates the two regions denoted I and IV in Fig. 4.

For $d < d_{\mathrm{DR}}(N)$, the fixed point controlling the critical behavior of the RF$O(N)$M must now be studied by keeping the full dependence on s of the renormalized disorder cumulant. We do find in this region that a cusp occurs at a finite time that corresponds to the Larkin scale discussed above. In Fig. 5, we illustrate the change in behavior related to the presence or absence of cusp in the fixed-point function $\delta_{*T}(\rho_{m,k}, s^2)$ for $N=3$. We plot $\delta_{*T}(\rho_{m,k}, s^2)$ as a function of both s^2 and d. Below some dimension 5.1, a cusp is clearly visible near $s=0$. We have checked its robustness and that it is indeed a

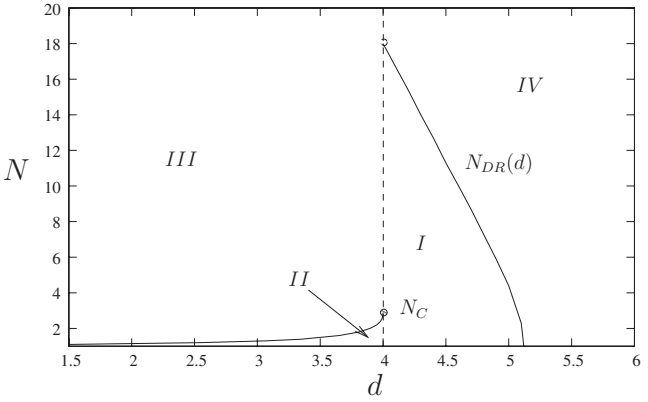

FIG. 4. Predicted phase diagram of the d-dimensional RF$O(N)$M. In region III, there are no phase transitions and the system is always disordered (paramagnetic). In regions I and IV, there is a second-order paramagnetic to ferromagnetic transition and in region *II*, a second-order transition between paramagnetic and QLRO phases. In region IV, the nonanalyticity of the effective action in the dimensionless field dependence at the zero-temperature fixed point is weak enough to let the critical exponents take their dimensional-reduction value, whereas a complete breakdown of dimensional reduction occurs in regions I and II.

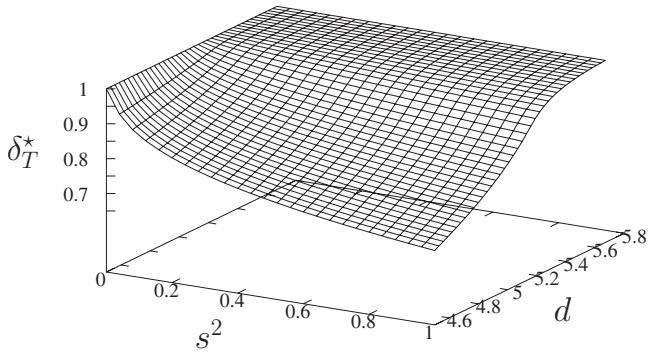

FIG. 5. Presence or absence of a cusp in the fixed-point function $\delta_{*T}(\rho_{m,k}, s^2)$ for $N=3$: two-dimensional plot of $\delta_{*T}(\rho_{m,k}, s^2)$ versus s^2 and d. Below some dimension around 5, a cusp is clearly visible near $s=0$.

behavior in $|s|$ by changing the spacing of the discretization of the s variable. The value of d for which the cusp first appears coincides with d_{DR} as previously determined from the divergence of $\partial^2_{s^2} v_k|_{\rho=\rho_{m,k}, s=0}$; here, $d_{\mathrm{DR}}(N=3) \simeq 5.1$.

Finally, we draw attention to the fact that the critical exponents continuously evolve upon crossing the critical line $d_{\mathrm{DR}}(N)$. This has been clearly illustrated in Fig. 1 for the exponents η and $\bar{\eta}$ near $d=4$: one can see that $\bar{\eta}$ gradually separates from η as N moves down from 18 and does *not* settle in general to the value $\bar{\eta} = 2\eta$. This provides strong evidence in favor of a characterization of the critical scaling behavior by three independent exponents and not two as suggested in Ref. 33.

C. Criticality, ferromagnetism, and quasi-long-range order

In the present NP-FRG formalism, the equilibrium phases of the system are characterized by the flow evolution of the dimensionless order parameter at scale k, $\rho_{m,k}$. Depending on the initial conditions, $\rho_{m,k}$ is found to (1) diverge when time goes to $-\infty$ $(k \to 0)$ in such a way that the dimensionful order parameter (the magnetization) tends to a finite value; this behavior can be associated with a fully stable (attractive) fixed point describing long-range ferromagnetic order, (2) go to zero at a finite scale, which corresponds to the disordered paramagnetic phase,[34] and (3) reach a nontrivial fixed-point value; the dimensionful order parameter which goes as $k^{d-4+\bar{\eta}} \rho_{m*}$ is then zero when $k=0$. In the latter case, if only one parameter (say, the initial value of $\rho_{m,k}$) need be adjusted, the fixed point is once unstable and describes the critical point of the model and the associated scaling behavior. This is the situation found in regions I and IV of the (N,d) diagram shown in Fig. 4 with, as discussed above, a qualitative difference with respect to dimensional reduction between the two regions.

A different pattern is found below dimension 4 for models with continuous symmetry $(N>1)$. Whatever the initial conditions, the RG flow no longer leads to a divergence of $\rho_{m,k}$, which is in line with the predicted absence of long-range order in the RF$O(N)$M for $d<4$. One obtains instead a nontrivial attractive fixed point characterized by a cusp in the second cumulant of the renormalized random field. This

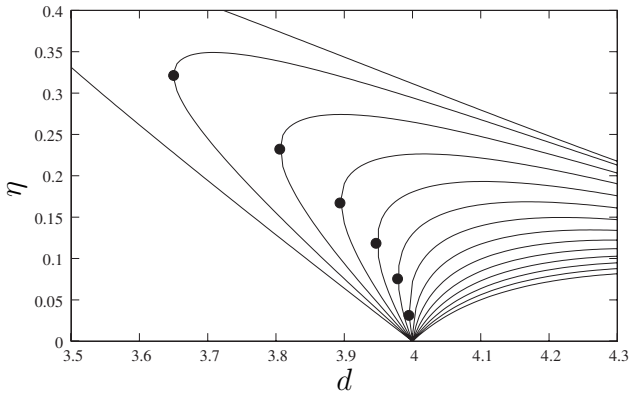

FIG. 6. Anomalous dimension η associated with the single or the two zero-temperature cuspy fixed points plotted versus d for values of N ranging from 1.4 to 4 by steps of 0.2. For $N>N_c \simeq 2.83$, only one fixed-point value emerges from the point $(\eta=0, d=4)$; but for $N<N_c$, one finds two values of η for each dimension, with the upper one being associated with the critical fixed point and the lower one with the QLRO fixed point. The two branches of fixed points coalesce for a value $d_{\rm lc}(N)$ shown by filled circles.

fixed point comes on top of the once unstable (critical) fixed point also characterized by a cusp. It describes a whole low-disorder phase that is associated with a nontrivial scaling behavior. This phase has a vanishing order parameter but algebraically decaying correlation functions characterized by the two anomalous dimensions η and $\bar{\eta}$ (see Sec. IVA of paper I). It therefore corresponds to a QLRO phase and it transforms into the disordered paramagnetic phase at a critical point itself controlled by a "cuspy" fixed point.

The QLRO phase only occurs below a critical value of the number of components, $N_c=2.83\cdots$, which can also be directly computed from an analysis of the perturbative FRG equations at and near $d=4$.[15,26,35] It is very similar to the QLRO phase found in elastic systems pinned by disorder,[8,10,11] and for the RFXYM($N=2$), it actually identifies to the latter phase when $d\to 4^-$. (The numerical solution of the truncated NP-FRG equations then reduces, as expected, to the one-loop perturbative FRG result for which the equivalence with a random periodic elastic model is easily shown; see, e.g., paper I.) However, contrary to the situation in disordered elastic systems, the QLRO phase only exists below a (bare) critical disorder and the existence of two cuspy fixed points provides a mechanism for destroying QLRO below some lower critical dimension.[15,26,35]

The variation with N and d of the characteristics of the two cuspy fixed points is illustrated in Fig. 6, where we plot the value of the anomalous dimension η versus d for a series of values of N. For $N>N_c\simeq 2.83$, only one fixed-point value emerges from the point $(\eta=0, d=4)$; but for $N<N_c$, one finds two values of η for each dimension: the upper one being associated with the critical fixed point and the lower one with the QLRO fixed point. One can see that the two fixed-point branches coalesce for a value $d_{\rm lc}(N)$ that consequently determines the lower critical dimension below which no phase transition is observed.

The lower critical dimension is shown in Fig. 4, where it separates region II with QLRO and region III with no phase transition. Note that the result is compatible with Feldman's prediction[36] that there is no QLRO above $N=3$. The lower critical curve, when seen as $N_{\rm lc}(d)$ in place of $d_{\rm lc}(N)$, decreases as d decreases and is expected to reach $N_{\rm lc}=1$ for $d=2$, which corresponds to the lower critical dimension (for long-range ferromagnetism) in the Ising version. [In our present approximate description, we find $N_{\rm lc}(d=2)\simeq 1.15$ instead of the exact result $N_{lc}=1$; see the discussion below.] This behavior is, in fact, reminiscent of what occurs in the pure $O(N)$ model.[15] Although never acknowledged, the (N,d) phase diagram of the latter, which is derived from the solution of phenomenological RG equations[37] and from known exact results, is indeed very similar to that of the RF$O(N)$M displayed in Fig. 4: the critical value N_c is now equal to 2 and occurs in $d=2$, which is the lower critical dimension for ferromagnetism; a QLRO phase exists in a region between $(N=1, d=1)$ and $(N=2, d=2)$, which is the counterpart of region II described above, but is, of course, not physically relevant for real systems. This QLRO is different from that associated with the low-temperature phase of the XY model in $d=2$, which is below the Kosterlitz–Thouless transition,[38,39] as the latter corresponds to a line of fixed points while the former is controlled by a single fixed point.

The situation found in the RF$O(N>1)$M below $d=4$ raises two questions. First, is a QLRO phase observable in an experimentally realizable random field system. The question is especially acute because it has been suggested that the $3-d$ RFXYM displays such a phase,[8,10,40] called Bragg glass in relation to pinned vortex lattices in disordered type-II superconductors. The second question is more academic and concerns the status of the singular point $(N_c=2.83,\ldots,d=4)$. Following the analogy with its counterpart $(N_c=2, d=2)$, in the pure $O(N)$ model (see above), one may wonder whether the random field model with $N_c=2.83\cdots$ in $d=4$ also gives rise to a Kosterlitz–Thouless transition. Elsewhere,[15,26] we have answered this question through an analysis of the perturbative FRG equations near $d=4$ at two loops, finding that there is no Kosterlitz–Thouless-type transition. A practical consequence of this result is that, as indeed reproduced by the numerical solution of the truncated NP-FRG equations, the critical line $N_{\rm lc}(d)$ abruptly drops with an infinite slope as one moves away from $d=4$ (see Fig. 4).

Going back now to the first question raised above, we conclude from looking at Fig. 4 that the $N=2$ RFXYM in $d=3$ is very distinctly in the region where no QLRO phase occurs. Therefore, we find that there is no Bragg glass in this model. This is confirmed by a direct study of our equations in $N=2, d=3$.[15] Here, as a cautionary note, we would like to point out that the absence of a Bragg-glass phase in the $3-d$ RFXYM does not necessarily imply that no such phase exists in disordered type-II superconductors. The relation between vortices in the latter systems and the RFXYM is derived via an "elastic glass model,"[10] and it does not guarantee that phase transitions associated with the presence of massive modes are identical in the two systems.

D. Robustness of the results

The results presented above rely on a nonperturbative, but approximate, RG description. It is therefore desirable to have

some estimate of its degree of accuracy. In addressing this point, we make use of the two main properties of the present NP-FRG formalism, which we have emphasized in several occasions in this paper and in paper I,

(1) *The existence of a systematic truncation scheme* that allows one to control and improve the results by going to higher orders of the truncation; this has been tested with success on the pure $O(N)$ model,[16,41,42] and we plan to do in the near future for the RF$O(N)$M (the calculations being, however, much more demanding).

(2) *A unified description of the whole* (N,d) plane for the d-dimensional RF$O(N)$M; one can therefore check the consistency of the approximate nonperturbative results by comparing to the known exact or perturbative results in the appropriate regions of the (N,d) plane. This is what we address in the following.

The numerical resolution of the truncated NP-FRG equations confirms the property, already stressed above and in paper I, that one recovers the one-loop perturbative predictions near $d=6$, when $N\to\infty$, and, more significantly, near $d=4$. A study of the two-loop perturbative FRG equations[15,26,35] near $d=4$ unambiguously supports the scenario found here concerning the presence of two nontrivial critical lines: one associated with the breaking of dimensional reduction, $N_{\mathrm{DR}}(d)$, which starts downward from $N=18$ when $d\to 4^+$, and one giving the lower critical dimension for QLRO below $d=4$, $N_{\mathrm{lc}}(d)$, which arrives at $N_c=2.83\cdots$ with an infinite slope when $d\to 4^-$. There are some quantitative differences (see Ref. 26), but the overall picture near $d=4$ is well captured by the present truncation.

To estimate the error made in locating the critical line $N_{\mathrm{DR}}(d)$, we have also considered a somewhat cruder approximation for the two-replica potential v_k, which is a plain expansion in powers of the fields (still around the minimum) including all terms up to φ^4,

$$\begin{aligned} v_k &= 2v_{1,k}(\sqrt{\rho_1\rho_2}z-\rho_{m,k})+v_{2,k}(\rho_1+\rho_2-2\rho_{m,k})^2 \\ &\quad + v_{3,k}(\rho_1-\rho_2)^2+v_{4,k}(\sqrt{\rho_1\rho_2}z-\rho_{m,k})^2 \\ &\quad + v_{5,k}(\sqrt{\rho_1\rho_2}z-\rho_{m,k})(\rho_1+\rho_2-2\rho_{m,k}), \end{aligned} \tag{32}$$

where $v_{1,k}=1$ by construction. The results (obtained from monitoring the divergence of $\partial^2_{|\boldsymbol{\varphi}_1-\boldsymbol{\varphi}_2|^2}v_k|_{\boldsymbol{\varphi}_1=\boldsymbol{\varphi}_2}$; see above) are very similar to those obtained with the more involved truncation: the critical line $N_{\mathrm{DR}}(d)$ starts again from $N=18$ near $d=4$ and extends down to $d_{\mathrm{DR}}\simeq 5$ when $N=1$. The value of $d_{\mathrm{DR}}(N=1)$ is found in the window 4.9–5.1, and it depends on the approximation and the choice of cutoff function.[43]

Finally, one may also compare the lower critical value $N_{\mathrm{lc}}(d)$ obtained when $d=2$ to the expected exact result, $N_{\mathrm{lc}}(d=2)=1$. As stated above, we find $N_{\mathrm{lc}}(d=2)\simeq 1.15$, which provides an estimate of the error. (The lower critical dimension of the RFIM is a difficult and unfavorable test for the present approach starting from a Ginzburg–Landau–Wilson bare action; as shown for the pure Ising model, the results can be improved by solving the full first order of the derivative expansion.[44])

The above discussion indicates that there is certainly room for improvement of the quantitative predictions (and we have provided a formalism to do so), but it also gives strong confidence in the robustness of the present description of the long-distance physics of the RF$O(N)$M.

V. PHYSICS OF THE CUSP AND ROLE OF TEMPERATURE

We devote this section to a discussion of the physics associated with the nonanalyticity found in the effective average action and of the role of temperature. To proceed, we build upon the body of work already done in the context of disordered elastic systems.[20,21,45–47] For ease of notation, we focus on the RFIM in the following, but most results will apply *mutatis mutandis* to the RF$O(N)$M.

A. Interpreting the cusp

Breakdown of dimensional reduction has been associated with the presence of multiple "metastable states," a metastable state being generically taken as a field configuration that minimizes some action or effective action. From the supersymmetric formalism of the RFIM,[5,48] one finds that a necessary condition for this breakdown is the existence of many *minima of the bare action* [as given by Eq. (1) of paper I]. In the present approach, on the other hand, the failure of dimensional-reduction predictions originates in a strong enough nonanalyticity in the dependence of the effective average action in the dimensionless field. To shed light on the connection between this nonanalyticity and a picture in terms of metastable states, we follow the line of reasoning developed for elastic systems pinned by a random potential.[20,21,45–47]

To begin with, it is worth stressing the unusual character of the RG analysis in the presence of a cusp. Generally speaking, integration over fluctuations, e.g., thermal fluctuations in statistical physics, smoothes away nonanalyticities as well as the effect of possible metastable states so that, at long distance, the effective average action is a nonsingular function of the dimensionless fields. The novelty in the RFIM case comes from the dominance of the (quenched) disorder fluctuations over the thermal ones and the associated property that the long-distance physics (criticality, ordering, and quasiordering) is controlled by zero-temperature fixed points. Actually, this physics is describable by directly working at zero temperature at all scales (see above and paper I). As argued in the context of disordered elastic systems,[19–21] integration over high-energy modes along the RG flow amounts at zero temperature to minimizing some coarse-grained action, and it is this minimization procedure that may lead to cusplike behavior in the presence of multiple minima in the coarse-grained action.

It is now instructive to go back to the interpretation of the two-replica potential $V_k(\phi_1,\phi_2)$ as the second cumulant of the renormalized disorder and of its second derivative $\Delta_k(\phi_1,\phi_2)$ as the second cumulant of the renormalized random field, both being evaluated for uniform field configurations (see paper I). To be more precise, the one-replica component of the effective average action $\Gamma_{k,1}[\phi]$ is the

Legendre transform of the first moment of the random free energy functional at scale k, $W_k[J;h]$, namely,

$$\Gamma_{k,1}[\phi] = -\overline{W_k[J;h]} + \int_x J(x)\cdot\phi(x), \tag{33}$$

where $J(x)$ is a linear source conjugate to the field $\phi(x)$ and the overbar denotes an average over quenched disorder, with h denoting the bare random field. On the other hand, the two-replica component is the second cumulant of $W_k[J;h]$ with $J \equiv J_k[\phi]$, where $J_k[\phi]$ is the nonrandom source defined via the above Legendre transform, i.e., $J_k[\phi](x) = \delta\Gamma_{k,1}[\phi]/\delta\phi(x)$. One therefore has

$$\Gamma_{k,2}[\phi_1,\phi_2] = \overline{\delta W_k[J_k[\phi_1];h]\delta W_k[J_k[\phi_2];h]}, \tag{34}$$

with $\delta W_k[J;h] = W_k[J;h] - \overline{W_k[J;h]}$.

One can also define a renormalized random field at the running scale k, $\breve{h}_k[\phi](x)$, as

$$\breve{h}_k[\phi](x) = -\frac{\delta}{\delta\phi(x)}\delta W_k[J[\phi];h]. \tag{35}$$

It has zero mean and its second cumulant is given by

$$\overline{\breve{h}_k[\phi_1](x)\breve{h}_k[\phi_2](y)} = \Gamma^{(11)}_{k,2,xy}[\phi_1,\phi_2]. \tag{36}$$

More details, including a discussion of higher-order cumulants, can be found in paper I.

Here, in the truncated NP-FRG considered, the random free energy functional $\delta W_k[J[\phi];h]$ is taken in a local approximation that amounts to replacing it by a random potential $\breve{V}_k(\phi;x)$ with zero mean and second cumulant,

$$\overline{\breve{V}_k(\phi_1;x)\breve{V}_k(\phi_2;y)} \simeq \delta(x-y)V_k(\phi_1,\phi_2). \tag{37}$$

Similarly, in this approximation, the renormalized random field defined above is given by $\breve{h}_k(\phi;x) = -\partial_\phi \breve{V}_k[\phi_1;x]$ with a second cumulant,

$$\overline{\breve{h}_k(\phi_1;x)\breve{h}_k(\phi_2;y)} \simeq \delta(x-y)\Delta_k(\phi_1,\phi_2). \tag{38}$$

All the above considerations, of course, apply to the dimensionless quantities, $v_k(\varphi_1,\varphi_2)$ and $\delta_k(\varphi_1,\varphi_2)$. In particular, one can introduce a dimensionless random potential $\breve{V}_k$ with its second cumulant given by $v_k(\varphi_1,\varphi_2)$ and an associated dimensionless random field with second cumulant given by $\delta_k(\varphi_1,\varphi_2)$. In what follows, we rather discuss the dimensionless functions since, at the fixed point, the dimensionful quantity V_k goes to zero whereas Δ_k diverges.

Following Ref. 21, a cusp in $\delta_*(\varphi_1,\varphi_2)$ as $\varphi_2 \to \varphi_1$ can be interpreted as resulting from a *cuspy random potential*. Such a potential is sketched in Fig. 7(a). It displays a sequence of minima separated by cusps located at random positions along the field axis. [The explicit spatial dependence of $\breve{v}_*(\varphi;x)$ has been dropped as, for instance, could be obtained from a properly rescaled integration over space.] As seen in Fig. 7(b), the dimensionless random field then shows discontinuities at those random locations, discontinuities that can be thought of as "shocks" through an analogy with the Burgers equation.[21,49]

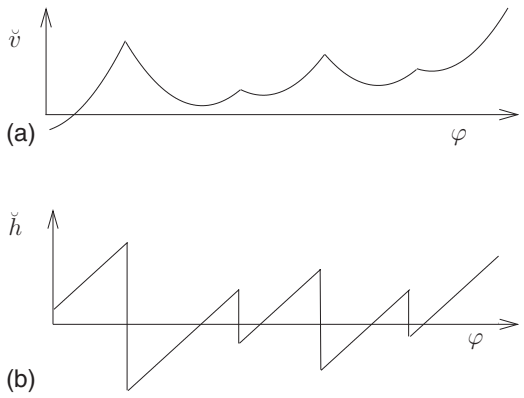

FIG. 7. Sketch of the field dependence of the dimensionless (a) renormalized random potential $\breve{v}_*(\varphi)$ and (b) random field $\breve{h}_*(\varphi) = -\partial_\varphi \breve{v}_*(\varphi)$ associated with a cusp in $\delta_*(\varphi_1,\varphi_2)$ as $\varphi_2 \to \varphi_1$. The cusps separating the minima in (a) correspond to discontinuities or shocks in (b); they are located at random positions along the field axis.

To see how the rugged cuspy landscape of Fig. 7(a) gives rise to a cusp in the second cumulant of the random field $\delta_*(\varphi_1,\varphi_2)$, consider the quantity $\overline{[\breve{h}_*(\varphi_1) - \breve{h}_*(\varphi_2)]^2}$ as $\varphi_2 \to \varphi_1$. Switching again to the variables $x = (\varphi_1+\varphi_2)/2$ and $y = (\varphi_1-\varphi_2)/2$, one has from Eq. (38),

$$\begin{aligned}\overline{[\breve{h}_*(\varphi_1) - \breve{h}_*(\varphi_2)]^2} &\simeq 2[\delta_*(x,0) - \delta_*(x,y)] \\ &\simeq -2\delta_{*,a}(x)|y| + O(y^2),\end{aligned} \tag{39}$$

where we have used the cusplike behavior as $y \to 0$ (see Sec. III B) and where $\delta_{*,a}(x)$ should be negative.

On the other hand, with a renormalized random field as pictured in Fig. 7(b), $\overline{[\breve{h}_*(\varphi_1) - \breve{h}_*(\varphi_2)]^2}$ is a $O(y^2)$ except when a discontinuity (shock) is present between the two fields φ_1 and φ_2. As a consequence,

$$\overline{[\breve{h}_*(\varphi_1) - \breve{h}_*(\varphi_2)]^2} \simeq \int_{x-|y|}^{x+|y|} dx_d \int d\gamma_d \overline{p(x_d,\gamma_d)}\gamma_d^2 + O(y^2), \tag{40}$$

where x_d is the shock location and γ_d is the amplitude of the associated discontinuity. Assuming that $\int d\gamma_d \overline{p(x,\gamma_d)}\gamma_d^2$ is nonzero, one indeed recovers Eq. (39) with $\delta_{*,a}(x) = -\int d\gamma_d \overline{p(x,\gamma_d)}\gamma_d^2$.

The above discussion therefore points to a picture in which, when dimensional reduction is broken, the fixed point controlling the critical behavior of the RFIM is described (for uniform field configurations) by a dimensionless random potential with multiple minima separated by cusps. These minima and the cuspy barriers separating them arrive along the RG flow because no minima are present in the random potential at the microscopic scale Λ. It is important to stress that this random potential is superimposed on a mean dimensionless potential $u_*(\varphi)$ which itself displays two equivalent minima at the fixed point. These global minima, which are located at the dimensionless fields $\pm\varphi_{m,*}$ (see above), characterize the incipient ferromagnetic ordering. Contrary to the

disordered elastic systems for which the random potential dominates at large scales over the elastic energy, the random potential in random field systems does control the (sample-to-sample) fluctuations, but never becomes predominant in the thermodynamic (mean) behavior. The long-distance behavior is determined by a subtle interplay between ferromagnetic ordering and randomness.

Finally, we mention that the rather elusive nature of the nonanalyticity in the effective average action may become more transparent when studied within a dynamic formalism. As pointed out by Chauve *et al.*,[45] the presence of a cusp may then be related to the existence of a nonzero threshold force below which the system stays trapped in a minimum of the random potential (metastable state). Again, this picture applies at zero temperature and it describes an out-of-equilibrium dynamic transition, namely the depinning of an elastic system in a random environment.[50] One may wonder if a similar relation exists in the RFIM between cusplike behavior and zero-temperature driven dynamics among metastable states: the analog of the depinning transition would then be an "avalanche transition" observed when driving the system by slowly varying an applied magnetic field (to use the terminology of magnetic materials in which the phenomenon is commonly observed).[51]

B. Role of temperature, droplet phenomenology, and activated dynamic scaling

Temperature, as has been stressed in several occasions in this paper and in paper I, plays a peculiar role in random field systems. It is irrelevant near the fixed points controlling criticality, ordering, and quasiordering. However, it is "dangerously irrelevant" in that, at nonzero temperature and slightly off the critical point, both static and dynamic quantities display somewhat anomalous scaling behavior coming from the scale dependence on the renormalized temperature.[18,52] To make contact with the discussion of Sec. V A, one may summarize the situation as follows:[46,47] the zero-temperature analysis provides information on the typical behavior of the system (including the typical fluctuations and correlation functions), as described by its ground state, whereas small nonzero temperature requires an account of rare events such as low-energy excitations. Metastable states play a role in both cases: rather intricate as far as the typical behavior is concerned (see above), more direct in the case of low-energy excitations. In the latter case, an efficient phenomenological approach has been proposed, known as the "droplet picture."[53,54]

In a nutshell, the droplet approach assumes the existence of rare samples (or rare regions in a sample) for which, on top of the ground state, an additional minimum (metastable state) is thermally accessible, the latter has an energy above the ground state of the order of the temperature. If one defines for a system of linear size L, sample-dependent (i.e., random) "connected," $\check{\chi}_c[h]$, and "disconnected," $\check{\chi}_d[h]$, susceptibilities as

$$\check{\chi}_c[h] = L^{-d} \int_x \int_y [\langle \chi(\boldsymbol{x})\chi(\boldsymbol{y})\rangle - \langle \chi(\boldsymbol{x})\rangle\langle \chi(\boldsymbol{y})\rangle] \tag{41}$$

and

$$\check{\chi}_d[h] = L^{-d} \int_x \int_y \langle \chi(\boldsymbol{x})\rangle\langle \chi(\boldsymbol{y})\rangle, \tag{42}$$

where $\chi(\boldsymbol{x})$ is the fundamental field in the bare action and the brackets denote a thermal average for a given configuration h of the bare random field (see Sec. IIA of paper I). At criticality and at a temperature T (criticality is attained by fine tuning the bare disorder strength whose critical value depends on T, as illustrated in Fig. 1 of paper I), most samples, which are characterized by a single populated minimum, are such that $\check{\chi}_d[h] \sim L^{4-\bar{\eta}}$ whereas, due to cancellation of the leading terms in Eq. (41), $\check{\chi}_c[h] \sim TL^{2-\eta}$. On the other hand, rare samples, which occur with a probability assumed to be of the order of $TL^{-\theta}$, where θ is the temperature exponent given by $\theta = 2 + \eta - \bar{\eta}$, have $\check{\chi}_d[h] \sim \check{\chi}_c[h] \sim L^{4-\bar{\eta}}$ (since the leading contributions to the two terms in $\check{\chi}_c[h]$ no longer cancel when two minima are populated). One therefore finds the following for the disorder-averaged pth moments:

$$\overline{\check{\chi}_c^p} \sim TL^{p(4-\bar{\eta})-\theta}, \tag{43}$$

$$\overline{\check{\chi}_d^p} \sim L^{p(4-\bar{\eta})}. \tag{44}$$

As a consequence, the fluctuations of the connected susceptibility are anomalous with, e.g., $\overline{\check{\chi}_c^2} \gg (\overline{\check{\chi}_c})^2$.

Another important prediction of the droplet approach concerns the dynamics of the RFIM near the critical point: the critical slowing down of the relaxation is shown to be "activated."[17,18,55] The typical relaxation time exponentially diverges as one approaches the critical point, with the effective activation barrier for relaxation diverging with system size as[18] L^{θ} at criticality.[56]

A major step toward formulating a fully consistent field theory and renormalization group framework for the droplet picture has been accomplished by Balents and Le Doussal[46,47,49,57] in the context of the random elastic model. The core of the connection between FRG formalism and droplet phenomenology is the existence of a "thermal boundary layer" that governs the highly nonuniform limit of the renormalized temperature going to zero. In the following, we do not attempt to provide an exhaustive description of thermal boundary layer and droplet picture in the RFIM, but rather stress some already illustrative results that we obtain within the minimal NP-FRG truncation.

To study the role of temperature in the NP-FRG formalism, we consider the flow equations for the RFIM, keeping now the terms depending on the renormalized temperature. From the results of Sec. IVB of paper I, one derives

$$-\partial_t u_k'(x) = \beta_{u'}^{T=0}(x) + 2v_d T_k l_1^{(d)}(u_k''(x))u_k'''(x), \tag{45}$$

$$
\begin{aligned}
&-\partial_t \delta_k(x,y) \\
&= \beta_\delta^{T=0}(x,y) + v_d T_k \Bigg\{ \frac{1}{2}[l_1^{(d)}(u_+'') + l_1^{(d)}(u_-'')]\delta_k^{(02)}(x,y) \\
&\quad - [l_2^{(d)}(u_+'')u_+''' - l_2^{(d)}(u_-'')u_-'''][\delta_k^{(01)}(x,y) + [l_1^{(d)}(u_+'') \\
&\quad - l_1^{(d)}(u_-'')]\delta_k^{(11)}(x,y)] + \frac{1}{2}[l_1^{(d)}(u_+'') + l_1^{(d)}(u_-'')] \\
&\quad \times \delta_k^{(20)}(x,y) - [l_2^{(d)}(u_+'')u_+''' + l_2^{(d)}(u_-'')u_-''']\delta_k^{(10)}(x,y) \Bigg\},
\end{aligned}
\tag{46}
$$

where $\beta_{u''}^{T=0}$ and $\beta_\delta^{T=0}$ are the $T=0$ beta functionals given by the right-hand sides of Eqs. (22) and (17), respectively, in which the running exponents η_k and $\bar{\eta}_k$ are now expressed at $T\neq 0$, and where $u_\pm'' \equiv u_k''(x \pm y)$ as in Eq. (17) (and similarly for $u_\pm'''$).

Taking the limit $y \to 0$ in Eq. (46) and allowing for cusp-like behavior, one finds for $\delta_{k,0}(x) = \delta_k(x, y=0)$ that

$$
\begin{aligned}
-\partial_t \delta_{k,0}(x) &= \beta_{\delta_0}|_{\mathrm{reg}}(x) - \frac{v_d}{2} l_2^{(d)}(u_k''(x))\partial_y^2 [\delta_k(x,y) \\
&\quad - \delta_{k,0}(x)]^2 \Big|_{y=0} + v_d T_k l_1^{(d)}(u_k''(x))\partial_y^2 \delta_k(x,y)|_{y=0}
\end{aligned}
\tag{47}
$$

with

$$
\begin{aligned}
\beta_{\delta_0}|_{\mathrm{reg}}(x) &= \beta_{\delta_0}^{T=0}|_{\mathrm{reg}}(x) + v_d T_k \{ l_1^{(d)}(u_k''(x))\delta_{k,0}''(x) \\
&\quad - 2 l_2^{(d)}(u_k''(x))\delta_{k,0}'(x) u_k'''(x) \},
\end{aligned}
\tag{48}
$$

and $\beta_{\delta_0}^{T=0}|_{\mathrm{reg}}$ is given by the right-hand side of Eq. (19).

If a cusp appears in the renormalized cumulant $\delta_k(x,y)$ near the fixed point, i.e., $\delta_k(x,y) = \delta_{k,0}(x) + |y|\,\delta_{k,a}(x) + O(y^2)$ as in Eq. (24), then the two anomalous terms appearing on the right-hand side of Eq. (47) behave quite differently: the term characteristic of the $T=0$ behavior, $\partial_y^2[\delta_k(x,y) - \delta_{k,0}(x)]^2|_{y=0}$, goes to $2\delta_{*,a}(x)^2$, whereas that proportional to T_k, $\partial_y^2 \delta_k(x,y)|_{y=0}$, blows up. For a fixed point to be reached and the theory to be renormalizable, the latter divergence must be canceled. The solution is that (i) there should be no cusp at finite T_k and (ii) convergence to the cuspy $T=0$ fixed-point function is nonuniform in y as $T_k \to 0$ and takes the form of a boundary layer.

In the close vicinity of the fixed point, when both y and T_k approach zero, one anticipates the following behavior:

$$
\delta_k(x,y) = \delta_{*,0}(x) + T_k f\left(x, \frac{y}{T_k}\right) + O(T_k^2),
\tag{49}
$$

where $\delta_{*,0}(x)$ is the $(T=0)$ fixed-point result for $y=0$, $f(x,\tilde{y})$ is a scaling function which is even in x and $\tilde{y}$ and analytic around $\tilde{y}=0$, and $O(T_k^2)$ denotes terms of order at least T_k^2 at fixed scaling variable $\tilde{y}$. With Eq. (49), the two anomalous contributions described above can be expressed as

$$
\partial_y^2[\delta_k(x,y) - \delta_{k,0}(x)]^2|_{y=0} = 2 f(x,0) f^{(02)}(x,0),
\tag{50}
$$

$$
T_k \partial_y^2 \delta_k(x,y)|_{y=0} = f^{(02)}(x,0),
\tag{51}
$$

with the same convention as before for the notation of partial derivatives. Inserting the above expressions into the flow equation for $\delta_k(x,y)$ [Eq. (46)], and using the fact that $\delta_{k,0}(x)$ is solution of the fixed-point equation at zero temperature for $y=0$, one finds up to a $O(T_k)$ that the scaling function f must satisfy that

$$
\frac{1}{2} l_2^{(d)}(u_*''(x))\partial_{\tilde{y}}^2[(x,\tilde{y}) - f(x,0)]^2 - l_1^{(d)}(u_*''(x)) f^{(02)}(x,\tilde{y})
\tag{52}
$$

is independent of $\tilde{y}$. The solution is easily obtained as

$$
\begin{aligned}
&f(x,\tilde{y}) - f(x,0) \\
&\quad = \frac{l_1^{(d)}(u_*''(x))}{l_2^{(d)}(u_*''(x))} \left[1 - \sqrt{1 - \left(\frac{l_2^{(d)}(u_*''(x)) f^{(02)}(x,0)}{l_1^{(d)}(u_*''(x))} \right) \tilde{y}^2 } \right],
\end{aligned}
\tag{53}
$$

where $f^{(02)}(x,0) < 0$ and $u_*''(x)$ is given by the fixed-point solution of Eq. (45). The zero-temperature cuspy fixed point is recovered by considering $y \neq 0$ and $T_k \to 0$, which leads to

$$
f(x, \tilde{y} \to \pm\infty) \sim \delta_{*,a}(x)|\tilde{y}|,
\tag{54}
$$

with $\delta_{*,a}(x) = f^{(02)}(x,0) < 0$. On the other hand, when $y \to 0$ at fixed $T_k \neq 0$, i.e., near $\tilde{y}=0$, $f(x,\tilde{y}) - f(x,0) = O(\tilde{y}^2)$. Equation (53) thus describes the rounding of the cusp near $y=0$ in a layer whose width of order T_k goes to zero as $k \to 0$.

We can now make contact with the droplet description of the RFIM. From the effective average action Γ_k, one has access to all Green's functions of the system via the $1-PI$ vertices (see paper I). In the present minimal truncation,

$$
\begin{aligned}
\Gamma_k[\{\phi_a\}] &= \int_{\boldsymbol{x}} \Bigg\{ \frac{1}{T} \sum_{a=1}^{n} \left[\frac{1}{2} Z_{m,k} |\partial \phi_a(\boldsymbol{x})|^2 + U_k(\phi_a(\boldsymbol{x})) \right] \\
&\quad - \frac{1}{2T^2} \sum_{a,b=1}^{n} V_k(\phi_a(\boldsymbol{x}), \phi_b(\boldsymbol{x})) \Bigg\},
\end{aligned}
\tag{55}
$$

where we use an explicit dependence on a bare temperature T for book-keeping purpose.

The $1-PI$ vertices are obtained by functional differentiation and their expression is given in Appendix B. When all fields are taken as uniform and, moreover, equal, the first vertices have the following form:

$$
\begin{aligned}
\Gamma^{(2)}_{k,(a,\boldsymbol{q}_1)(b,\boldsymbol{q}_2)}(\{\phi_f = \phi\}) &= (2\pi)^d \delta(\boldsymbol{q}_1 + \boldsymbol{q}_2) \{ \delta_{ab} \hat{\Gamma}_k^{(2)}(\phi; q_1) \\
&\quad + \tilde{\Gamma}_k^{(2)}(\phi, \phi; q_1) \},
\end{aligned}
\tag{56}
$$

$$
\Gamma^{(3)}_{k,(a,\boldsymbol{q}_1)(b,\boldsymbol{q}_2)(c,\boldsymbol{q}_3)}(\{\phi_f = \phi\}) = (2\pi)^d \delta(\boldsymbol{q}_1 + \boldsymbol{q}_2 + \boldsymbol{q}_3) \Gamma^{(3)}_{k,abc}(\phi),
\tag{57}
$$

$$
\begin{aligned}
&\Gamma^{(4)}_{k,(a,\boldsymbol{q}_1)(b,\boldsymbol{q}_2)(c,\boldsymbol{q}_3)(d,\boldsymbol{q}_4)}(\{\phi_f = \phi\}) \\
&\quad = (2\pi)^d \delta(\boldsymbol{q}_1 + \boldsymbol{q}_2 + \boldsymbol{q}_3 + \boldsymbol{q}_4) \Gamma^{(4)}_{k,abcd}(\phi),
\end{aligned}
\tag{58}
$$

where the functions $\hat{\Gamma}_k^{(2)}(\phi; q)$, $\tilde{\Gamma}_k^{(2)}(\phi, \phi; q)$, $\Gamma^{(3)}_{k,abc}(\phi)$, and

$\Gamma^{(4)}_{k,abcd}(\phi)$ can be derived from Eqs. (B1)–(B3).

The (connected) Green's functions may be obtained from the replicated free energy functional $W_k[\{J_a\}]$, which is the Legendre transform of the effective average action $\Gamma_k[\{\phi_a\}]$. The procedure consists of using the standard formulas that relate the $W_k^{(p)}$'s to the $\Gamma_k^{(p)}$'s (Ref. 58) and expanding both sides in number of free replica sums as explained in paper I, keeping only the leading terms. This is detailed in Appendix B. The Green's functions can be cast in a form similar to that of the $1-PI$ vertices, namely, for equal field arguments,

$$W^{(2)}_{k,(a,\boldsymbol{q}_1)(b,\boldsymbol{q}_2)}(\{\phi_f=\phi\}) = (2\pi)^d\delta(\boldsymbol{q}_1+\boldsymbol{q}_2)\Big\{\delta_{ab}\hat{G}^{(2)}_k(\phi;q_1) + \tilde{G}^{(2)}_k(\phi,\phi;q_1) + O\Big(\sum_f\Big)\Big\}, \quad (59)$$

$$W^{(3)}_{k,(a,\boldsymbol{q}_1)(b,\boldsymbol{q}_2)(c,\boldsymbol{q}_3)}(\{\phi_f=\phi\}) = (2\pi)^d\delta(\boldsymbol{q}_1+\boldsymbol{q}_2+\boldsymbol{q}_3)G^{(3)}_{k,abc}(\phi;\boldsymbol{q}_1,\boldsymbol{q}_2), \quad (60)$$

$$W^{(4)}_{k,(a,\boldsymbol{q}_1)(b,\boldsymbol{q}_2)(c,\boldsymbol{q}_3)(d,\boldsymbol{q}_4)}(\{\phi_f=\phi\}) = (2\pi)^d\delta(\boldsymbol{q}_1+\boldsymbol{q}_2+\boldsymbol{q}_3+\boldsymbol{q}_4)G^{(4)}_{k,abcd}(\phi;\boldsymbol{q}_1,\boldsymbol{q}_2,\boldsymbol{q}_3), \quad (61)$$

where the various quantities appearing in the right-hand sides are related to the $1-PI$ counterparts in Eqs. (56)–(58) as discussed in Appendix B. Note that in the present truncation of the effective average action (limited to the first order of the derivative expansion),[13] information on the Green's functions is essentially limited to zero external momenta, more precisely external momenta with $|\boldsymbol{q}|$ less than the running scale k. Thanks to the RG framework, this is enough to provide a determination of the anomalous dimension of the field η, but in what follows, we only consider the case of external momenta set to zero.

Next, focusing on the critical (scaling) region, we introduce dimensionless functions and fields by using the scaling dimensions suitable for a zero-temperature fixed point (see Sec. II); so, for instance,

$$\frac{1}{T}U''_k(\phi) \simeq \frac{k^{4-\bar{\eta}}}{T_k}u''_*(\varphi), \quad (62)$$

$$\frac{1}{T^2}\Delta_k(\phi_1,\phi_2) \simeq \frac{k^{4-\bar{\eta}}}{T_k^2}\delta_k(\varphi_1,\varphi_2). \quad (63)$$

In addition, we eventually take the limit of equal field arguments in all expressions after insertion of the results obtained for the thermal boundary layer description of $\delta_k(\varphi_1,\varphi_2)$ [Eqs. (49) and (53)].

In the scaling region, the Green's functions at zero external momenta can then be expressed as

$$\hat{G}^{(2)}_k(\phi;0) \simeq T_k k^{-(4-\bar{\eta})}h^{(2)}_*(\varphi), \quad (64)$$

$$\tilde{G}^{(2)}_k(\phi,\phi;0) \simeq k^{-(4-\bar{\eta})}g^{(2)}_*(\varphi), \quad (65)$$

$$G^{(3)}_{k,abc}(\phi;\mathbf{0},\mathbf{0}) \simeq k^{-(d/2)-(3/2)(4-\bar{\eta})}\{g^{(3)}_*(\varphi) + T_k h^{(3)}_*(\varphi)(\delta_{ab}+\delta_{bc}+\delta_{ca}) + O(T_k^2)\}, \quad (66)$$

$$G^{(4)}_{k,abcd}(\phi;\mathbf{0},\mathbf{0},\mathbf{0}) \simeq k^{-d-2(4-\bar{\eta})}\Big\{g^{(4)}_*(\varphi) + T_k h^{(4)}_*(\varphi) \times(\delta_{ab}+\delta_{ac}+\delta_{ad}+\delta_{bc}+\delta_{bd}+\delta_{cd}) + T_k\frac{f^{(02)}(\varphi,0)}{u''_*(\varphi)^4}[\delta_{abc}+\delta_{abd}+\delta_{acd}+\delta_{bcd} - (\delta_{ab}\delta_{cd}+\delta_{ac}\delta_{bd}+\delta_{ad}\delta_{bc})] + O(T_k^2)\Big\}, \quad (67)$$

where $\phi\to 0$ (as $k^{(d-4+\bar{\eta})/2}\varphi$) and where the functions $g^{(p)}_*(\varphi)$ and $h^{(p)}_*(\varphi)$, $p=2,3,4,...$, are obtained from $u''_*(\varphi)$ and $\delta_{*,0}(\varphi)$ and their derivatives. Their expression is not particularly illuminating and we do not reproduce them here; see Appendix B for more details.

From the definition of the replicated generating functional $W_k[\{J_a\}]$, one can derive the relation between the replica Green's functions considered above and the physical Green's functions directly defined in the disordered system.[13] Still working at the running scale k and at zero external momenta, the first moments of the (random) connected and disconnected susceptibilities introduced in Eqs. (41) and (42) are, for instance, given by

$$\overline{\breve{\chi}_{k,c}} = \hat{G}^{(2)}_k(\phi;0), \quad (68)$$

$$\overline{\breve{\chi}_{k,d}} = \tilde{G}^{(2)}_k(\phi,\phi;0), \quad (69)$$

whereas the second moments read

$$\overline{\breve{\chi}^2_{k,c}} = k^d[G^{(4)}_{k,aabb}(\phi) - 2G^{(4)}_{k,aabc}(\phi) + G^{(4)}_{k,abcd}(\phi)], \quad (70)$$

$$\overline{\breve{\chi}^2_{k,d}} = k^d G^{(4)}_{k,abcd}(\phi), \quad (71)$$

where distinct replica indices here mean distinct replicas (no summation implied).

Setting together all the above results [Eqs. (64)–(71)], we find that the moments of the random disconnected susceptibility scale as

$$\overline{\breve{\chi}_{k,d}} \sim k^{-(4-\bar{\eta})}, \quad (72)$$

$$\overline{\breve{\chi}^2_{k,d}} \sim k^{-2(4-\bar{\eta})}, \quad (73)$$

whereas those of the random connected susceptibility scale as

$$\overline{\breve{\chi}_{k,c}} \sim T_k k^{-(4-\bar{\eta})} \sim T k^{-(2-\eta)}, \quad (74)$$

$$\overline{\breve{\chi}^2_{k,c}} \sim -T_k k^{-2(4-\bar{\eta})}\frac{f^{(02)}(\varphi,0)}{u''_*(\varphi)^4} \sim T k^{-2(4-\bar{\eta})+\theta}, \quad (75)$$

where we have used that $T_k\sim Tk^{\theta}$, and we recall that $f^{(02)}(\varphi,0)=\delta''_{*,a}(\varphi)<0$. Notice that only the term due to the

boundary layer appears in Eq. (75) (the other contributions cancel out).

From this analysis, we therefore obtain that the moments of the random connected and disconnected susceptibilities in the truncated NP-FRG precisely scale as in the droplet description: compare Eqs. (72)–(75) and Eqs. (43) and (44), with $L \sim k^{-1}$. The anomalous scaling of the moments of the connected susceptibility, which is due to rare low-energy excitations in the droplet picture, results in the NP-FRG from the presence of a thermal boundary layer in the vicinity of the zero-temperature fixed point, as illustrated by Eq. (75). This is in complete agreement with the more detailed analysis performed in Ref. 47 for disordered elastic systems.

To conclude this section, we briefly address the question of the slowing down of the relaxation toward equilibrium near the critical point. At long times, the dynamics of the RFIM can be modeled by a Langevin equation,

$$\partial_\tau \chi(\boldsymbol{x},\tau) = -\Omega \frac{\delta S[\chi;h]}{\delta \chi(\boldsymbol{x},\tau)} + \zeta(\boldsymbol{x},\tau), \tag{76}$$

where τ denotes the physical time (to be distinguished from the RG time t) and $\zeta(\boldsymbol{x},\tau)$ is a thermal noise taken with a Gaussian distribution characterized by a zero mean and a second moment,

$$\overline{\zeta(\boldsymbol{x},\tau)\zeta(\boldsymbol{y},\tau')} = 2T\Omega\,\delta(\tau-\tau')\,\delta(\boldsymbol{x}-\boldsymbol{y}). \tag{77}$$

In Eq. (76), $S[\chi;h]$ is the bare action for the RFIM, with h being the bare random field (see for instance Sec. II of paper I), and Ω is a kinetic coefficient that describes the bare relaxation rate and sets the elementary time scale in the problem. (We consider here the case of a nonconserved order parameter,[59] but the case of a conserved order parameter could also be of interest.[60])

An RG formalism can be conveniently implemented by using standard field theoretical techniques to build the generating functional of the time-dependent correlation and response functions.[58,61–63] Associated with this functional is a "bare dynamic action" that depends on two fields: the fundamental field and a "response" field. The average over the quenched disorder can now be performed without introducing replicas. By a Legendre transform, one then introduces an "effective dynamic action" that is the generating functional of the disorder-averaged, time-dependent $1-PI$ vertices.

In this setting, one can repeat the steps detailed in paper I to construct a NP-FRG approach to the dynamics: add a masslike regulator with an infrared cutoff function that suppresses the contribution of low-momentum and low frequency modes, define a (dynamic) effective average action at scale k, whose evolution with k is governed by an exact RG flow equation, and devise a truncation scheme.[64] In the present problem, this latter step can be done in the spirit of the minimal truncation considered above and in paper I. One, however, needs an additional assumption concerning the time dependence that, similarly to the spatial dependence, can be handled via an appropriate "derivative expansion," The simplest approximation that captures the physics is a "single time scale" approximation in which one introduces a single renormalized relaxation rate Ω_k. (This parallels the single wave function renormalization parameter used to describe the spatial dependence of the field in the minimal truncation; see paper I.)

From the boundary layer structure and by analogy with the previous work on the random elastic model,[45,47] one then expects that the renormalized relaxation rate flows as

$$\partial_t \ln(\Omega_k) \sim -T_k^{-1} \tag{78}$$

near the zero-temperature fixed point. This indeed corresponds to activated dynamic scaling and fits in with the droplet picture summarized above. A proper derivation of this result and an account of the (expected) broad distribution of relaxation rates would require a detailed dynamic treatment, but this goes beyond the scope of the present paper.

VI. CONCLUSION AND PERSPECTIVES

In this paper, which is the second part of a series of articles reporting our work on a NP-FRG approach for random field models and related disordered systems, we have applied the formalism presented in paper I to the d-dimensional random field $O(N)$ model. We have focused on two main issues related to the long-distance physics of the model: the breakdown of the dimensional-reduction property predicted by conventional perturbation theory and the nature of the phase diagram and ordering transitions in the (N,d) plane.

Within our NP-FRG approach, the way out of dimensional reduction is the appearance of a strong enough nonanalyticity in the dependence of the effective average action in the dimensionless field near the relevant zero-temperature fixed point. We have shown that this occurs below a critical dimension $d_{\mathrm{DR}}(N)$, which continuously goes from $N_{\mathrm{DR}}=18$ as $d \to 4^+$ to $d_{\mathrm{DR}} \simeq 5$ for $N=1$. In addition, we provide a description of criticality, ferromagnetic ordering, and quasi-long range order in the whole (N,d) plane. The NP-FRG method is able to directly address the phase diagram of the model in low (physical) dimension d and small (physical) number of components N: in particular, we find that there is no Bragg-glass phase, i.e., no phase with quasi-long range order in the three-dimensional RFXYM. Note that all those results are made possible by the very structure of the present RG approach that is (1) functional, (2) approximate but nonperturbative, and (3) devised to provide a continuous and consistent description of the whole plane of N,d.

Building upon earlier work on random elastic models,[46,47] we have also shown how the NP-FRG formalism gives access to both the typical behavior of the system, which is controlled by zero-temperature fixed points with a nonanalytic effective action, and to the physics of rare low-energy excitations ("droplets"), which is described at nonzero temperature by the rounding of the nonanalyticity in a thermal boundary layer.

Work still remains to be done for a complete understanding of random field models. We have pointed in several occasions in this paper and in the preceding one that clarifying the putative link between breaking of the underlying supersymmetry[5] and appearance of a nonanalyticity in the effective action would require to "upgrade" the present NP-

FRG formalism to a superfield formulation of the random field models. We defer this, as well as the study of improved nonperturbative truncations, to a forthcoming publication. We have also indicated an interesting extension of the present work to the dynamics of the RFIM, both to the out-of-equilibrium driven dynamics at zero temperature and to the (activated) relaxation to equilibrium at nonzero temperature. Finally, the connection to the proposed picture of the RFIM in terms of "spontaneous replica symmetry breaking" and "replica bound states"[65–68] remains to be investigated.

The NP-FRG formalism appears as a powerful tool to study random field models and related disordered systems. Whether such an approach can be generalized to tackle another major unsettled problems of the field of disordered systems, the long-distance physics of spin glasses, is a challenging but completely open question.

ACKNOWLEDGMENTS

We thank D. Mouhanna for helpful discussions.

APPENDIX A: NONANALYTICITY IN THE RANDOM FIELD ISING MODEL NEAR $d=6$

Our starting point is the RG flow equations for $\delta_{k,0}(x)$ and $\delta_{k,2p}(x)$ obtained by assuming that $\delta_k(x,y)$ is regular enough near $y=0$ [see Eqs. (19)–(21)]. The linear operators appearing in those equations are given by

$$L_{2p}[u'',\delta_0,\delta_2] = -[p(d-4+\bar{\eta}_k)+2\eta_k-\bar{\eta}_k]-\frac{1}{2}(d-4+\bar{\eta}_k)x\partial_x+2v_d\Big\{l_2^{(d)}(u''(x))\,\delta_0(x)\partial_x^2+2(p+1)[l_2^{(d)}(u''(x))\,\delta_0'(x)$$
$$-2l_3^{(d)}(u''(x))\,\delta_0(x)u_k'''(x)]\partial_x+\frac{p(2p+3)+1}{2}[l_2^{(d)}(u''(x))\,\delta_0''(x)-2l_3^{(d)}(u''(x))\,\delta_0'(x)u_k'''(x)$$
$$+2l_4^{(d)}(u''(x))\,\delta_0(x)u_k'''(x)^2]-\frac{p(2p+3)}{2}l_2^{(d)}(u''(x))\,\delta_2(x)\Big\} \tag{A1}$$

for $p\geq 2$; the expression of $L_2[u'',\delta_0]$ is obtained by setting $p=1$ in the above equation and dropping the last term so that $\delta_2(x)$ no longer appears in the operator. Note that, as for the threshold functions (see paper I), there is an explicit dependence on k due to η_k and $\bar{\eta}_k$ that comes on top of the dependence that may occur through the arguments.

Near $d=6$, one finds, as developed in Sec. VA of paper I, that the fixed point is characterized by $\eta_*=\bar{\eta}_*=O(\epsilon^2)$, $u_*''(x)=\epsilon(\lambda_{1*}/2)(3x^2-x_{m*}^2)+O(\epsilon^2)$, and $\delta_*(x,y)=1+\epsilon^2 d(x,y)$, with $x_{m*}^2=6v_6 l_2^{(6)}(0)$, $\lambda_{1*}=[36v_6 l_3^{(6)}(0)]^{-1}$, and $d(x,y)=O(1)$. The result for $\delta_*(x,y)$ implies that $\delta_{*,0}'(x)=O(\epsilon^2)$ and $\delta_{*,2p}(x)=O(\epsilon^2)$.

After inserting these results in Eq. (A1), one obtains that for $p=O(1)$,

$$L_{2p*}(x) \simeq -2p-x\partial_x+2v_d l_2^{(d)}(0)\partial_x^2+O(\epsilon) \tag{A2}$$

at the fixed point. We have made the implicit assumption, whose consistency can be checked, that the derivatives with respect to x acting on the $\delta_{k,2p}$'s do not modify the order in ϵ. The eigenfunctions of the above linear operator (with the condition that they are bounded by polynomials at large values of the argument[69]) are the Hermite polynomials $H_n(x/\sqrt{4v_d l_2^{(d)}(0)})$ (Ref. 70) with associated eigenvalues $\lambda_{2p,n}=-(2p+n)$, with $n\in\mathbb{N}$. Recalling that the RG time t in Eq. (21) goes to $-\infty$ as $k\to 0$, the above result means that the corresponding directions are irrelevant on approaching the fixed point. (This confirms the result found in Sec. VA of paper I that the fixed point given above is once unstable at first order in ϵ.)

However, a new phenomenon may appear when p is very large and scales as $1/\epsilon^2$. In this case, one finds that

$$L_{2p*}(x) \sim -2p\Big\{1-\frac{v_d}{4}p[2l_4^{(d)}(0)u_*'''(x)^2$$
$$+l_2^{(d)}(0)[\delta_{0*}''(x)-\delta_{2*}(x)]]+O(\epsilon)\Big\}, \tag{A3}$$

where the whole second term in the braces is of order 1 and, if positive, can become larger than 1 for some value of p so that L_{2p*} becomes positive.

To analyze the sign of L_{2p*}, one has to study $\delta_{0*}''(x)$ and $\delta_{2*}(x)$ at order ϵ^2. This is easily performed from Eqs. (19) and (20). One finds that $\delta_{0*}''(x)=-\delta_{2*}(x)=18v_d l_4^{(d)}(0)\lambda_{1*}^2\epsilon^2$, which indeed guarantees that the second term in the right-hand side of Eq. (A3) is positive. Evaluating L_{2p*} for $x=x_{m*}$ and using the expression of $u_*'''(x)$ now gives

$$L_{2p*}(x_{m*}) \sim -2p\{1-K^2(p\epsilon^2)+O(\epsilon)\}, \tag{A4}$$

with $K=l_2^{(d)}(0)l_4^{(d)}(0)/[6l_3^{(d)}(0)]^2$. One therefore concludes that for $p\gtrsim 1/(K\epsilon)^2$ $L_{2p*}(x_{m*})$ becomes positive, which, according to Eq. (21), leads to a divergence of $\delta_{k,2p}(x_{m*})$ as $k\to 0$. As a consequence, the renormalized disorder cumulant displays a subcusp of order $1/\epsilon^2$ at the fixed point. A related phenomenon has also been proposed by Feldman.[25]

APPENDIX B: GREEN'S FUNCTIONS IN THE TRUNCATED NONPERTURBATIVE FUNCTIONAL RENORMALIZATION GROUP OF THE RFIM

The $1-PI$ vertices are obtained by functional differentiation of the truncated effective average action given in Eq. (55). For uniform field configurations, one finds

$$\Gamma^{(2)}_{k,(a,\boldsymbol{q}_1)(b,\boldsymbol{q}_2)}[\{\phi_f\}] = (2\pi)^d \delta(\boldsymbol{q}_1+\boldsymbol{q}_2)\left\{ \delta_{ab}\frac{1}{T}[Z_{m,k}q_1^2 + U_k'(\phi_a)] - \frac{1}{T^2}\Delta_k(\phi_a,\phi_b)\right\}, \tag{B1}$$

$$\Gamma^{(3)}_{k,(a,\boldsymbol{q}_1)(b,\boldsymbol{q}_2)(c,\boldsymbol{q}_3)}[\{\phi_f\}] = (2\pi)^d \delta(\boldsymbol{q}_1+\boldsymbol{q}_2+\boldsymbol{q}_3)\left\{ \frac{\delta_{abc}}{T}U_k'''(\phi_a) - \frac{1}{2T^2}[\delta_{ab}\Delta_k^{(10)}(\phi_b,\phi_c) + \mathrm{perm}(abc)]\right\}, \tag{B2}$$

$$\Gamma^{(4)}_{k,(a,\boldsymbol{q}_1)(b,\boldsymbol{q}_2)(c,\boldsymbol{q}_3)(d,\boldsymbol{q}_4)}[\{\phi_f\}] = (2\pi)^d \delta(\boldsymbol{q}_1+\boldsymbol{q}_2+\boldsymbol{q}_3+\boldsymbol{q}_4)\left\{ \frac{\delta_{abcd}}{T}U_k''''(\phi_a) - \frac{1}{2T^2}[\delta_{abc}\Delta_k^{(20)}(\phi_c,\phi_d) + \mathrm{perm}(abcd)] - \frac{1}{2T^2}[\delta_{ab}\delta_{cd}\Delta_k^{(11)}(\phi_a,\phi_c) + \delta_{ac}\delta_{bd}\Delta_k^{(11)}(\phi_a,\phi_d) + \delta_{ad}\delta_{bc}\Delta_k^{(11)}(\phi_a,\phi_c)]\right\}, \tag{B3}$$

where $\delta_{abc} \equiv \delta_{ab}\delta_{bc}$, $\delta_{abcd} \equiv \delta_{ab}\delta_{bc}\delta_{cd}$, "perm$(abc)$" denotes the two terms obtained by circular permutations of the indices abc, and "perm$(abcd)$" denotes the three terms obtained by circular permutations of the indices $abcd$. All other notations are as in paper I and above.

The connected Green's functions $W^{(p)}_{k,(a_1,\boldsymbol{q}_1)\ldots(a_p,\boldsymbol{q}_p)}(\{\phi_f\})$ are related to the $1-PI$ vertices by formulas deriving from the Legendre transform between W_k and Γ_k.[58] For instance, the two-point connected Green's function $W_k^{(2)}$ is the inverse of the two-point $1-PI$ vertex, $\boldsymbol{W}_k^{(2)} = \boldsymbol{\Gamma}_k^{(2)-1}$. By using the expansion in number of free replica sums detailed in Sec. IID of paper I, one obtains at leading order

$$W^{(2)}_{k,(a,\boldsymbol{q}_1)(b,\boldsymbol{q}_2)}[\{\phi_f\}] = (2\pi)^d \delta(\boldsymbol{q}_1+\boldsymbol{q}_2)\left\{ \delta_{ab}\hat{G}_k^{(2)}(\phi_a;q_1) + \tilde{G}_k^{(2)}(\phi_a,\phi_b;q_1) + O\left(\sum_f\right)\right\}, \tag{B4}$$

where $O(\Sigma_f)$ denotes higher orders in the expansion in number of free replica sums, and with

$$\hat{G}_k^{(2)}(\phi_a;q) = \frac{T}{Z_{m,k}q^2 + U_k''(\phi_a)}, \tag{B5}$$

$$\tilde{G}_k^{(2)}(\phi_a,\phi_b;q) = \frac{\Delta_k(\phi_a,\phi_b)}{(Z_{m,k}q^2 + U_k''(\phi_a))(Z_{m,k}q^2 + U_k''(\phi_b))}. \tag{B6}$$

The three- and four-point connected Green's functions are derived along similar lines by using the standard graphical representation[58] and keeping the lowest order in the expansion in free replica sums.

Consider now the scaling region. As discussed in the main text around Eqs. (62) and (63), one can introduce dimensionless quantities and use the results concerning the thermal boundary layer. For the $1-PI$ vertices evaluated at zero external momenta and for equal field arguments, one explicitly obtains the expressions of the functions $\hat{\Gamma}_k^{(2)}$, $\tilde{\Gamma}_k^{(2)}$, $\Gamma^{(3)}_{k,abc}$, and $\Gamma^{(4)}_{k,abcd}$ appearing in Eqs. (56) and (58),

$$\hat{\Gamma}_k^{(2)}(\phi;q=0) \simeq \frac{k^{4-\bar{\eta}}}{T_k}u_*''(\varphi), \tag{B7}$$

$$\tilde{\Gamma}_k^{(2)}(\phi,\phi;q=0) \simeq -\frac{k^{4-\bar{\eta}}}{T_k^2}\delta_{*,0}(\varphi), \tag{B8}$$

$$\Gamma^{(3)}_{k,abc}(\phi) \simeq \frac{k^{4-\bar{\eta}-21/2(d-4+\bar{\eta})}}{T_k} \times\left\{ \delta_{abc}u_*'''(\varphi) - \frac{\delta_{*,0}'(\varphi)}{2T_k}(\delta_{ab}+\delta_{bc}+\delta_{ca})\right\}, \tag{B9}$$

$$\Gamma^{(4)}_{k,abcd}(\phi) \simeq \frac{k^{4-\bar{\eta}-(d-4+\bar{\eta})}}{T_k}\left\{ \delta_{abcd}u_*''''(\varphi) - \frac{\delta_{*,0}''(\varphi)}{4T_k}[\delta_{abc}+\delta_{bcd} + \delta_{cda}+\delta_{dab}+\delta_{ab}\delta_{cd}+\delta_{ac}\delta_{bd}+\delta_{ad}\delta_{bc}] - \frac{f^{(02)}(\varphi,0)}{4T_k^2}[\delta_{abc}+\delta_{bcd}+\delta_{cda}+\delta_{dab} - (\delta_{ab}\delta_{cd}+\delta_{ac}\delta_{bd}+\delta_{ad}\delta_{bc})]\right\}, \tag{B10}$$

where of course, the dimensionful field ϕ vanishes (as $k^{(d-4+\bar{\eta})/2}$).

Inserting the above equations in the expressions of the connected Green's functions, Eqs. (B4)–(B6) and their generalizations for higher-order functions, finally leads to Eqs. (64)–(67) of the text, with, for instance,

$$g_*^{(2)}(\varphi) = \delta_{*,0}(\varphi)u_*''(\varphi)^{-2}, \tag{B11}$$

$$h_*^{(2)}(\varphi) = u_*''(\varphi)^{-1}, \tag{B12}$$

etc. As stated in the text, the expressions for the other functions $g_*^{(p)}(\varphi)$ and $h_*^{(p)}(\varphi)$, $p=3,4,\ldots$, only involve $u_*''(\varphi)$ and $\delta_{*,0}(\varphi)$ and their derivatives. Obtaining them is tedious but straightforward, and the resulting formulas are not worth displaying.

*Present address: Instituto de Física, Facultad de Ingenería, Universidad de la República, J. H. y Reissig 565, 11000 Montevideo, Uruguay. tissier@lptmc.jussieu.fr
†tarjus@lptl.jussieu.fr

[1] Y. Imry and S. K. Ma, Phys. Rev. Lett. **35**, 1399 (1975).
[2] A. Aharony, Y. Imry, and S. K. Ma, Phys. Rev. Lett. **37**, 1364 (1976).
[3] G. Grinstein, Phys. Rev. Lett. **37**, 944 (1976).
[4] A. P. Young, J. Phys. C **10**, L257 (1977).
[5] G. Parisi and N. Sourlas, Phys. Rev. Lett. **43**, 744 (1979).
[6] J. Z. Imbrie, Phys. Rev. Lett. **53**, 1747 (1984).
[7] J. Bricmont and A. Kupiainen, Phys. Rev. Lett. **59**, 1829 (1987).
[8] T. Giamarchi and P. Le Doussal, Phys. Rev. Lett. **72**, 1530 (1994).
[9] G. Blatter, M. V. Feigel'man, V. B. Geshkenbern, A. I. Larkin, and V. M. Vinokur, Rev. Mod. Phys. **66**, 1125 (1994).
[10] T. Giamarchi and P. Le Doussal, Phys. Rev. B **52**, 1242 (1995).
[11] T. Giamarchi and P. Le Doussal, *Spin Glasses and Random Fields* (World Scientific, Singapore, 1998), p. 321.
[12] T. Nattermann and S. Scheidl, Adv. Phys. **49**, 607 (2000).
[13] G. Tarjus and M. Tissier, preceding paper, Phys. Rev. B **78**, 024203 (2008).
[14] G. Tarjus and M. Tissier, Phys. Rev. Lett. **93**, 267008 (2004).
[15] M. Tissier and G. Tarjus, Phys. Rev. Lett. **96**, 087202 (2006).
[16] J. Berges, N. Tetradis, and C. Wetterich, Phys. Rep. **363**, 223 (2002).
[17] J. Villain, Phys. Rev. Lett. **52**, 1543 (1984).
[18] D. S. Fisher, Phys. Rev. Lett. **56**, 416 (1986).
[19] D. S. Fisher, Phys. Rev. Lett. **56**, 1964 (1986).
[20] L. Balents and D. S. Fisher, Phys. Rev. B **48**, 5949 (1993).
[21] L. Balents, J. P. Bouchaud, and M. Mézard, J. Phys. I **6**, 1007 (1996).
[22] P. Le Doussal, K. J. Wiese, and P. Chauve, Phys. Rev. B **66**, 174201 (2002).
[23] P. Le Doussal, K. J. Wiese, and P. Chauve, Phys. Rev. E **69**, 026112 (2004).
[24] D. S. Fisher, Phys. Rev. B **31**, 7233 (1985).
[25] D. E. Feldman, Phys. Rev. Lett. **88**, 177202 (2002).
[26] M. Tissier and G. Tarjus, Phys. Rev. B **74**, 214419 (2006).
[27] The correlation length exponent ν is still given, however, by its dimensional-reduction value, $\nu=1/\epsilon$, but this is no longer true at the next (two-loop) order in ϵ (see Ref. 26).
[28] Cuspy fixed points are also present when $N>18$, but they are more than once unstable and correspond to possible multicritical behavior (see Refs. 26 and 71).
[29] A. I. Larkin, Sov. Phys. JETP **31**, 784 (1970).
[30] A. I. Larkin and Y. N. Ovchinnikov, J. Low Temp. Phys. **34**, 409 (1979).
[31] G. Tarjus and M. Tissier (unpublished).
[32] D. Litim, Phys. Lett. B **486**, 92 (2000).
[33] M. Schwartz, J. Phys. C **18**, 135 (1985).
[34] In the present truncation that relies on an expansion around a nontrivial minimum, i.e., different from zero, we do not pursue the study of the flow once $\rho_{m,k}$ reaches zero; if one is interested in investigating the disordered phase, it is not difficult to change the truncation (see Ref. 72). Note also that generically the disordered (symmetric) fixed points are not at zero temperature.
[35] P. Le Doussal and K. J. Wiese, Phys. Rev. Lett. **96**, 197202 (2006).
[36] D. E. Feldman, Phys. Rev. B **61**, 382 (2000).
[37] J. L. Cardy and H. W. Hamber, Phys. Rev. Lett. **45**, 1217 (1980).
[38] J. M. Kosterlitz and D. J. Thouless, J. Phys. C **6**, 1181 (1973).
[39] V. L. Berezinskii, Sov. Phys. JETP **32**, 493 (1970).
[40] M. J. P. Gingras and D. A. Huse, Phys. Rev. B **53**, 15193 (1996).
[41] L. Canet, B. Delamotte, D. Mouhanna, and J. Vidal, Phys. Rev. D **67**, 065004 (2003).
[42] L. Canet, B. Delamotte, D. Mouhanna, and J. Vidal, Phys. Rev. B **68**, 064421 (2003).
[43] In addition, one should keep in mind that the dimensional-reduction fixed point is only approximately described in the minimal truncation (see paper I) and that the exponents η and $\bar{\eta}$ slightly deviate from the dimensional-reduction prediction as one moves away from $d=4$ and from $d=6$.
[44] H. Ballhausen, J. Berges, and C. Wetterich, Phys. Lett. B **582**, 144 (2004).
[45] P. Chauve, T. Giamarchi, and P. Le Doussal, Phys. Rev. B **62**, 6241 (2000).
[46] L. Balents and P. Le Doussal, Europhys. Lett. **65**, 685 (2004).
[47] L. Balents and P. Le Doussal, Ann. Phys. (N.Y.) **315**, 213 (2005).
[48] G. Parisi, in *Proceedings of Les Houches 1982, Session XXXIX*, edited by J. B. Zuber and R. Stora (North Holland, Amsterdam, 1984), p. 473.
[49] P. Le Doussal, Europhys. Lett. **76**, 457 (2006).
[50] D. S. Fisher, Phys. Rev. B **31**, 1396 (1985).
[51] K. A. Dahmen, J. P. Sethna, and O. Perkovic, in *The Science of Hysteresis*, edited by G. Bertotti and I. Mayergoyz (Elsevier, Amsterdam, 2005), p. 107.
[52] J. Villain, J. Phys. (Paris) **46**, 1843 (1985).
[53] A. J. Bray and M. A. Moore, J. Phys. C **17**, L463 (1984).
[54] D. S. Fisher and D. A. Huse, Phys. Rev. B **38**, 373 (1988).
[55] D. S. Fisher and D. A. Huse, Phys. Rev. B **38**, 386 (1988).
[56] This behavior is quite different from conventional critical slowing down for which the relaxation time diverges as a power law described by a critical exponent z (Ref. 59).
[57] L. Balents and P. Le Doussal, Phys. Rev. E **69**, 061107 (2004).
[58] J. Zinn-Justin, *Quantum Field Theory and Critical Phenomena*, 3rd ed. (Oxford University Press, New York, 1989).
[59] P. C. Hohenberg and B. I. Halperin, Rev. Mod. Phys. **49**, 435 (1977).
[60] D. A. Huse, Phys. Rev. B **36**, 5383 (1987).
[61] P. C. Martin, E. D. Siggia, and H. A. Rose, Phys. Rev. A **8**, 423 (1973).
[62] C. De Dominicis, J. Phys. C **1**, 247 (1976).
[63] H. K. Janssen, Z. Phys. B **23**, 377 (1976).
[64] B. Delamotte and L. Canet, Condens. Matter Phys. **8**, 163 (2005).
[65] M. Mézard and A. P. Young, Europhys. Lett. **18**, 653 (1992).
[66] C. De Dominicis, H. Orland, and T. Temesvari, J. Phys. I **5**, 987 (1995).
[67] E. Brézin and C. De Dominicis, Eur. Phys. J. B **19**, 467 (2001).
[68] G. Parisi and N. Sourlas, Phys. Rev. Lett. **89**, 257204 (2002).
[69] T. R. Morris, Prog. Theor. Phys. Suppl. **131**, 395 (1998).
[70] *Handbook of Mathematical Functions*, edited by M. Abramowitz and I. A. Stegun (Dover, New York, 1964).
[71] Y. Sakamoto, H. Mukaida, and C. Itoi, Phys. Rev. B **74**, 064402 (2006).
[72] N. Tetradis and C. Wetterich, Nucl. Phys. B: Field Theory Stat. Syst. **422**[FS], 541 (1994).